OpenNano 11 (2023) 100138

Contents lists available at ScienceDirect

OpenNano

journal homepage: www.elsevier.com/locate/onano

Review article

Nanotheranostics to target antibiotic-resistant bacteria: Strategies and applications

Rahul Bhattacharjee [a,1], Arvind Negi [b,1,*], Basudha Bhattacharya [a,1], Tanima Dey [a], Priya Mitra [a], Subham Preetam [c], Lamha Kumar [d], Sulagna Kar [a], Sabya Sachi Das [e,1], Danish Iqbal [f], Mehnaz Kamal [g], Fayez Alghofaili [h], Sumira Malik [i], Abhijit Dey [j], Saurabh Kumar Jha [k], Shreesh Ojha [l], Ana Cláudia Paiva-Santos [m,n], Kavindra Kumar Kesari [b,o,*], Niraj Kumar Jha [k,p,q,*]

[a] KIIT School of Biotechnology, Kalinga Institute of Industrial Technology (KIIT-DU), Bhubaneswar, Odisha, India
[b] Department of Bioproducts and Bio-systems, School of Chemical Engineering, Aalto University, Espoo 00076, Finland
[c] Institute of Advanced Materials, IAAM, Gammalkilsvägen 18, Ulrika, 59053, Sweden
[d] School of Biology, Indian Institute of Science Education and Research, Thiruvananthapuram, India
[e] School of Pharmaceutical and Population Health Informatics, DIT University, Dehradun 248009, Uttarakhand, India
[f] Department of Health Information Management, College of Applied Medical Sciences, Buraydah Private Colleges, Buraydah 51418, Saudi Arabia
[g] Department of Pharmaceutical Chemistry, College of Pharmacy, Prince Sattam Bin Abdulaziz University, Al-Kharj 11942, Saudi Arabia
[h] Department of Medical Laboratory Sciences, College of Applied Medical Sciences, Majmaah University, Majmaah 11952, Saudi Arabia
[i] Amity Institute of Biotechnology, Amity University Jharkhand, Ranchi, Jharkhand, 834001, India
[j] Department of Life Sciences, Presidency University, 86/1 College Street, Kolkata, 700073, West Bengal, India
[k] Department of Biotechnology, School of Engineering and Technology, Sharda University, Knowledge Park III, Greater Noida, Uttar Pradesh, India
[l] Department of Pharmacology and Therapeutics, College of Medicine and Health Sciences, United Arab Emirates University, Al Ain P.O. Box 15551, United Arab Emirates
[m] Department of Pharmaceutical Technology, Faculty of Pharmacy of the University of Coimbra, University of Coimbra, Coimbra, Portugal
[n] REQUIMTE/LAQV, Group of Pharmaceutical Technology, Faculty of Pharmacy of the University of Coimbra, University of Coimbra, Coimbra, Portugal
[o] Department of Applied Physics, School of Science, Aalto University, Espoo 00076, Finland
[p] Department of Biotechnology, School of Applied & Life Sciences (SALS), Uttaranchal University, Dehradun 248007, India
[q] School of Bioengineering and Biosciences, Lovely Professional University, Phagwara 144411, Punjab, India

Abbreviations: CDC, Centers for Disease Control and Prevention; WHO, World Health Organization; XDR-TB, Extensively drug-resistant TB; MDR-TB, Multidrug-resistant tuberculosis; PM, Plasma membrane; NPs, Nanoparticles; TLR, Toll-like receptors; PAMP, Pathogen-associated molecular patterns; TRIF, TIR-domain-containing adapter-inducing interferon-β; Ni, Nickle; TiO_2, Titanium oxide; ZnO, Zinc oxide; ZrO_2, Zirconium oxide; AgNP, Silver nanoparticles; LPS, Lipopolysaccharide; K, Potassium; M1, Inflammatory phenotype; M2, Anti-inflammatory phenotype; GO, Graphene oxide; PMNs, Polymorphonuclear leukocytes; NETs, Neutrophil extracellular traps; APC, Antigen-presenting cells; MHC, Major histocompatibility complex; FeO, Ferric oxide; SPR, Surface Plasmon Resonance; LSPR, Localized Surface Plasmon Resonance; PDT, Photodynamic therapy; PDI, Protein Disulfide Isomerase; HSV, Herpes simplex virus; CN, Chitin nanofibrils; PHAs, Polyhydroxyalkanoates; PHACOS, PHAs integrated with sulfur groups, and thioester moieties; PMs, Polymeric micelles; PMMA, Poly(methyl methacrylate); MIF, Migratory inhibitory factor; PDMAEMA, Poly (2-N, N-dimethyl aminoethyl methacrylate); MDA, Malondialdehyde; GSH, Glutathione; MRSA, Methicillin-resistant Staphylococcus aureus; MLV, Murine Leukemia Virus; LUV, Unilamellar vesicles; HA-OLA, Hyaluronic acid-oleylamine; AMPs, Antimicrobial peptide polymers; SNAPPs, Structurally nanoengineered antimicrobial peptide polymers; MNMs, Molecular nanomachines; ROS, Reactive oxygen species; AuNPs, Gold nanoparticles; AZM, Azithromycin; CLR, Clarithromycin; MIC, Minimum inhibitory concentration.

* Corresponding author at: Department of Biotechnology, School of Engineering & Technology (SET) Sharda University, Knowledge Park III, Greater Noida, Uttar Pradesh-201310, India.

E-mail addresses: arvind.negi@helsinki.fi, arvind.negi@aalto.fi (A. Negi), kavindra.kesari@aalto.fi (K.K. Kesari), niraj.jha@sharda.ac.in (N.K. Jha).

[1] Authors have contributed equally.

https://doi.org/10.1016/j.onano.2023.100138
Received 27 June 2022; Received in revised form 22 February 2023; Accepted 3 March 2023
Available online 5 March 2023

ARTICLE INFO

Keywords:
Nano-sized materials
Antibacterial
Antibiotic drug resistance
Nano-device
Nano-robots
Nano-antibiotics
Nano-materials

ABSTRACT

Various health agencies, such as the European Medical Agency (EMA), Centers for Disease Control and Prevention (CDC), and World Health Organization (WHO), timely cited the upsurge of antibiotic resistance as a severe threat to the public health and global economy. Importantly, there is a rise in nosocomial infections among covid-19 patients and in-hospitalized patients with the delineating disorder. Most of nosocomial infections are related to the bacteria residing in biofilm, which are commonly formed on material surfaces. In biofilms, microcolonies of various bacteria live in syntropy; therefore, their infections require a higher antibiotic dosage or cocktail of broad-spectrum antibiotics, aggravating the severity of antibiotic resistance. Notably, the lack of intrinsic antibacterial properties in commercial-grade materials desires to develop newer functionalized materials to prevent biofilm formation on their surfaces. To devise newer strategies, materials prepared at the nanoscale demonstrated reasonable antibacterial properties or enhanced the activity of antimicrobial agents (that are encapsulated/chemically functionalized onto the material surface). In this manuscript, we compiled such nanosized materials, specifying their role in targeting specific strains of bacteria. We also enlisted the examples of nanomaterials, nanodevice, nanomachines, nano-camouflaging, and nano-antibiotics for bactericidal activity and their possible clinical implications.

1. Introduction

Exponential growth in the human population substantially increases the demand for food products and the utilization of antibiotics in agricultural practices and dairy products [1]. Furthermore, the number of patients receiving immune therapies and implants has drastically increased in the last decade, amplifying antibiotic usage [2,3]. Additionally, poorly practiced [4] antibiotics usage in low-income regions (for example, Asia-Pacific, Africa, and South America) [5] has threatened the antibiotic sector and shifted the interest of major global pharmaceuticals from antibiotics toward conventional areas (such as cancer, diabetes, cardiovascular diseases) [6]. Such a paradigm shift in the drug research market can be observed by comparing the drugs approved by the FDA in the last 40 years [7]. In this period of 2015–21, shrinkage of the antibiotic sector was evident as FDA-approved anticancer (29%) and neurological disorders (12%), while only 14% were infectious drugs, which is alarming low considering the plethora of pathogens causing human diseases (such as viruses, bacteria, fungi, and protozoa) [8]. The encounter with new bacterial strains which carry antibiotic-resistance genes (such as multidrug-resistant (MDR) or extensively drug-resistant strains (XDR)) challenges healthcare and poses a severe threat to the global economy. However, in-hospital patients who receive surgical implants or suffer from delineating disorders are at high risk of developing secondary infections (called "nosocomial infections"). Most nosocomial infections originate from the bacteria residing in biofilms. Biofilms are commonly found on potable water piping and various household types of equipment. According to the CDC, approximately 687,000 cases and 72,000 fatalities were recorded with nosocomial infections in the United States in 2015 alone [9]. To exacerbate the situation, residing bacteria in biofilms possesses acquired genes than their freely suspended cellular form. Therefore, a higher dosage or cocktail of antibiotics is typically required to treat such infections, ultimately increasing the risk of evolving antibiotic-restraint strains and affecting the microbial ecology (as shown in Fig. 1).

Typical bacterial infections are common in human societies and, therefore, effectively managed with a regular body immune response or eradicated with broad-spectrum antibiotics. The mechanism of these antibiotics is to either limit the overgrowing bacteria population ("bacteriostatic) by diminishing the essential protein or alter the gene responsible for carrying out the metabolism, which affects the growth of bacteria. While the other way, these antibiotics work as bactericidal, where specific enzymes or signaling pathways get targeted, limiting the particular metabolite biosynthesis essential for bacteria survival [10]. Although a few antibiotics have shown clinical efficiency for the biofilm-based secondary infections in hospitalized patients with delineating disorders (such as covid-19, cancer, heart problems, and liver and kidney malfunctioning), but as these bacteria possess altered metabolism and genetic representation, therefore, complete eradication of their infection takes prolong treatments and higher dosage of antibiotics. Such treatment aggravates the risk of the emergence of multidrug resistance and jeopardizes gut microbes' physiology [11]. These antibiotic regimes inhibit intracellular signaling proteins (or enzymes), hamper the nucleic acid synthetic pathways (DNA or RNA), and suppress cell wall formation. However, these antibiotics gradually lose their therapeutic efficacy after prolonged use as bacteria mutate their gene in such a way that brings structural changes in the respective intracellular protein (or enzyme), restricting the binding conformation of antibiotics [12]. Such bacteria generally showedMDR specific genes. For example, *mecA* mutations lead to resistance to beta-lactam drugs (methicillin-resistant *Staphylococcus aureus*, MRSA); *Delhimetallo-b-lactamase-1* (NDM-1) mutations commonly found in gram-negative bacteria, makes bacteria resistant to a broad range of beta-lactam antibiotics [13]. These MDR strains of bacteria are manifested with distinctive characteristics, such as decreased cellular uptake of antibiotics, modulating the intra-membrane channels [14], sustaining effluxing pump to expel antibiotics [15], hydrolysis of the antibiotics (highly cited in the case of beta-lactam antibiotics), mutations in the other intracellular machinery (protein, enzyme or cellular accessories). Mutations in intracellular target is a common reason for MDR as it alters the specific amino acid in the active binding cavity of the target protein, thereby abolishing the binding of drugs. For example, methicillin resistance is acquired due to the production of a penicillin-binding

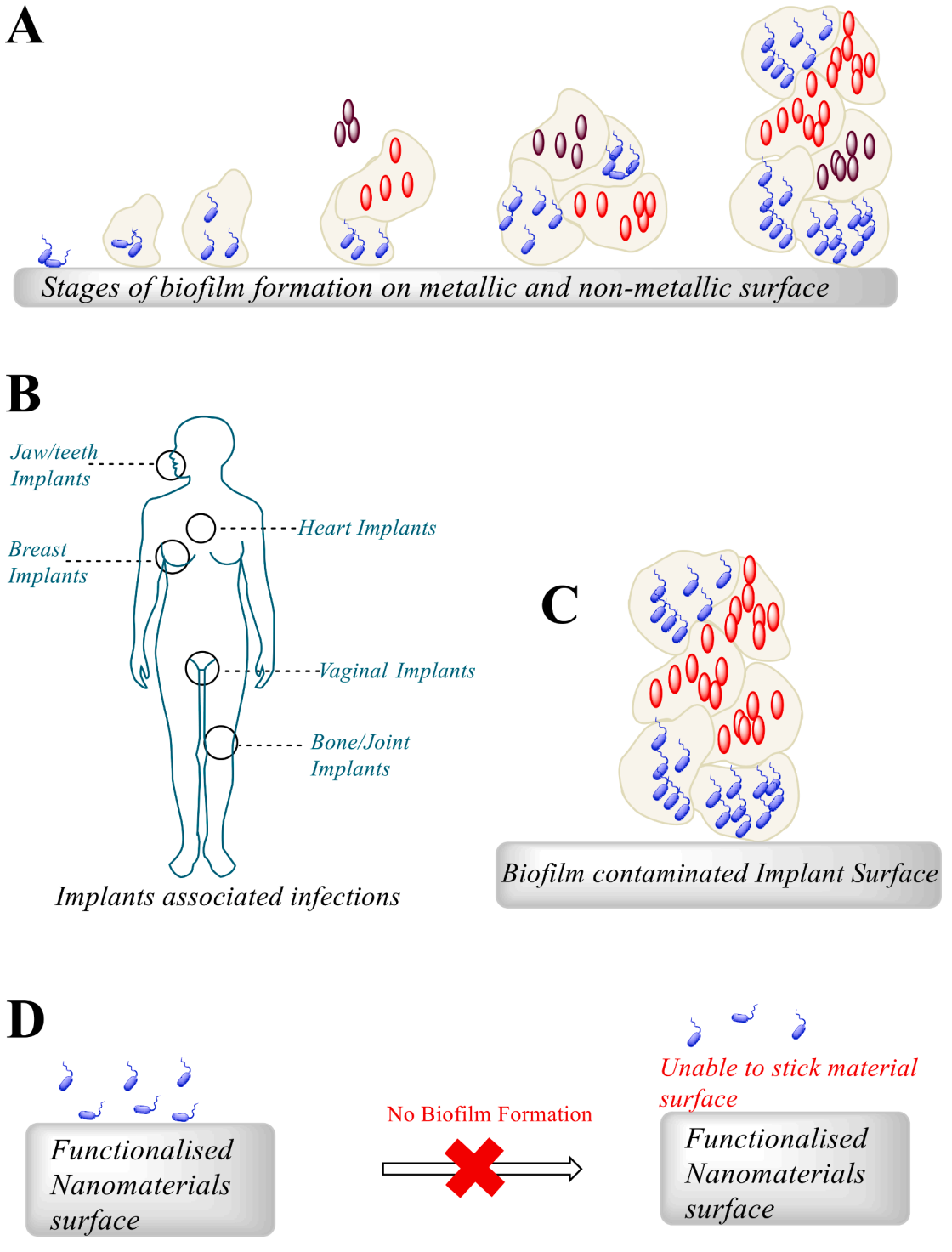

Fig. 1. (A) Various stages of microbial biofilm formation on the material surface, (B) Implants associated with biofilm contamination, (C) Biofilm formation on the surface of a material, and (D) Application of functionalized nanomaterial surfaces to prevent microbial biofilm formation [8].

protein that binds to all β-lactams with poor affinity and even bacterial cell develops alternative metabolic pathways to by-pass the effect of antibiotics [16]. Therefore, clincal treatments for the infections originated from MDR and XDR bacteria strains becoming difficult because of their genetic evolution and requires either identifying new antimicrobial drugs for mutated intracellular targets or druggable targets. However, identification of new antimicrobial and druggable targets, requires a huge investment and takes years of development, therefore innovative approaches has been implemented to address the infections of MDR and XDR bacteria. Strategies

involving nanoparticles (NPs) as potential antibacterials have increasing demand due to their superior physicochemical characteristics and facile access to their experimental setups [17,18]. These nanoparticle-based strategies commonly enhance the physiochemical aspects of engaged antibiotics, increasing their kinetic rates of absorption and distribution. Such changes in the physicochemical properties of antibiotics amplify their mode of action, thereby exhibiting improved antibacterial effects [19]. Common clinical implications of NPs strategies, such as (a) NPs as a vehicle for the administration of existing anti-MDR antibiotics [20,21]; (b) NPs based drug-delivery carrier system for controlled drug release, allowing targeted antibiotics delivery for the penetration of the biofilm against microorganisms [22]; (c) NP-based antimicrobial exhibit lesser toxicity and sustained therapeutic efficacy [23]. Therefore, we have compiled various NPs strategies, either in the advanced developmental phase or preliminary stages of their implementation. However, one of the shortcomings that NPs strategies often face is the impaired acute immune response cells after their delivery, leading to their short life in the systemic circulation. Therefore, we also discussed the influence of these nanoparticle-based strategies against host immunity.

2. Impact of nano-strategies on host immunity

Direct clinical use of nano-based strategies as a single antimicrobial agent poses certain limitations, including immune response, allergic reactions (if administered through the skin), limited systemic circulation time, and limited bioavailability. In addition, although NPs exhibit reasonable *in vitro* antimicrobial activity, their *in vivo* administration remains challenging due to a commonly reciprocated host immune response [24,25]. To an extent, immune responses against NPs can be minimized by modifying the physical features of NPs (such as size, shape, surface charge, surface topology, stability, solubility, and crystallization) [26,27]. However, the immune system's complexity rejected such clinical implications of nanotheranostics. To date, a complete interactive cellular model of innate and adaptive immune systems with NPs is still understudied; however, reports that featured those critical studies are illustrated in Fig. 2.

2.1. Impact of nanotheranostics on TLR signaling of innate immunity

TLRs are the type-I transmembrane receptors that identify PAMP and recruit a specific group of adaptor molecules with the TIR domain, such as MyD88 and TRIF, to begin downstream signaling cascades that result in the production of inflammatory type-I IFN and chemokines [28]. Ni-NPs is an inorganic activator that binds with TLR to trigger inflammation responses [29]. Moreover, the metal-based NPs (TiO_2, ZnO, ZrO_2, Ag) were involved in TLR signaling inflammation. TiO_2 and ZrO_2 NPs elevated TLR-10 and TLR-7 mRNA levels in human macrophages and TLR2 and TLR4 mRNA in mouse liver cells [30,31]. Also, TLR-3 and TLR-9 ligand-induced IL-6 production in murine macrophages was increased by tiopronin (*2-mercaptopropionylglycine*) capped-silver NPs [32]. ZnO-NPs are also known to trigger MyD88-dependent proinflammatory cytokines through the TLR signaling pathway [33], whereas quantum dots activate MyD88-dependent TLR (at the surface of the cell or inside of the cell), initiating inflammatory response [34]. Smaller NPs interact with TLRs through LPS binding proteins to activate cascade for TLR signaling, while larger NPs directly bind to TLRs [35]. External stimuli, including silica, aluminum crystals, and asbestos, induce an innate inflammatory response, which the inflammasomes recognize [36–40]. The inflammasome is a family of multi-protein complexes activated by bacterial toxins and foreign materials (such

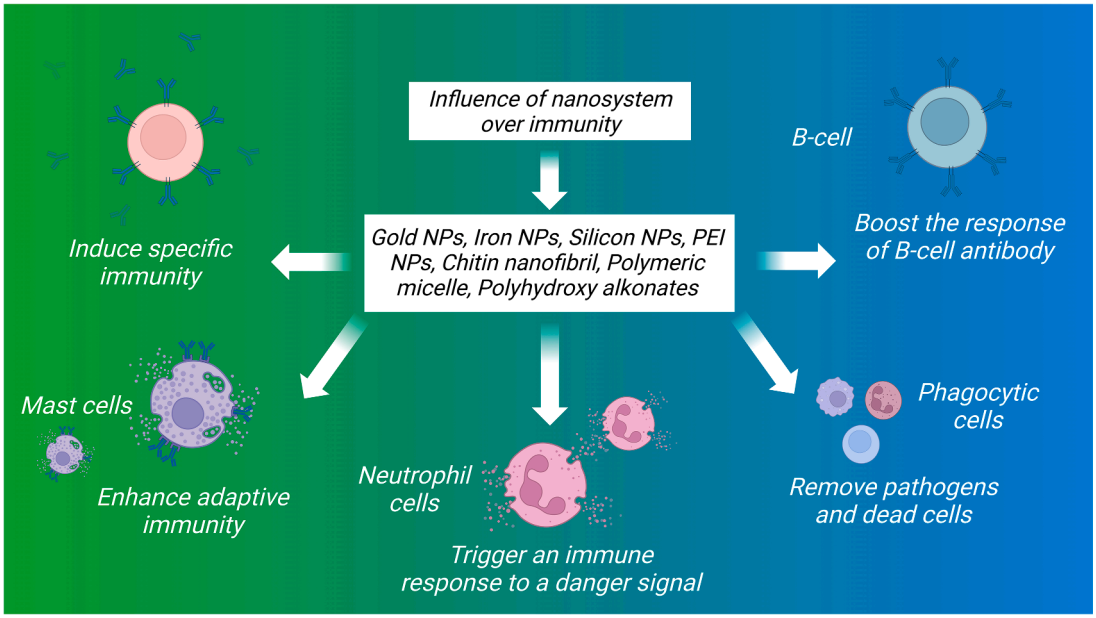

Fig. 2. Cellular model showing the interaction of nanotheranostics with specific immune cells.

as silica, aluminum, or calcium pyrophosphate crystals) [41]. NP-induced inflammasome activation is invariably associated with pyroptosis. For example, carbon black NPs cause pyroptosis [42]. Endotoxin-free hollow carbon spheres induce the NLRP3-ASC-caspase-1-dependent IL-1 production in macrophages in humans without cytotoxicity [43]. The presence of NPs was found to downregulate the inflammatory response against external stimuli. When NPs interact with the host immune system, they interrupt the TLR signaling pathway, reducing bacteria's ability to stimulate innate immune responses.

2.2. *Impact of nanotheranostics on macrophage polarization*

Macrophages and monocytes play an essential role in maintaining the host's immune defense against infection by initiating the inflammatory response and coordinating the repair of tissues, which causes remodeling and supports the development and homeostasis of tissues [44–46]. Macrophages have excellent phagocytic properties in eliminating foreign particles that impair the tissues' physiological and functional integrity. The surrounding microenvironment induces macrophages' plasticity and functional phenotypes at various stages of an inflammatory reaction *via* an inflammatory phenotype (M1) or an anti-inflammatory phenotype (M2). M1 is associated with defense against infection, whereas M2 is responsible for immunosuppression and tissue remodeling [47,48]. NPs are foreign particles that enter the host body and get eliminated *via* M2 macrophages, which are activated, differentiated, and polarized [49,50]. There are limited resources discussing the effect of NPs on macrophage polarization and its molecular mechanisms (as shown in Fig. 3). Physiochemical features of NPs, including surface, size, and chemical composition, could modulate polarization and reprogramming of the macrophages. Furthermore, the same NPs elicit polarization of macrophages in various ways depending on the length of exposure or the amount used for stimulation. Metal NPs (Ag-NPs and Au-NPs) directly produce M1 polarization, while Au-NPs are more effective than Ag-NPs [51]. Metal oxide NPs (e.g., AgO, ZnO, TiO_2) also stimulate M1 inflammatory cytokines release in a dose-dependent manner [52]. The chemical composition of ceramic NPs (SiO_2, TiO_2, and ZrO_2) appears to affect macrophage polarization. SiO_2 NPs cause the polarization of macrophages towards an M1 phenotype, but ZrO_2 and TiO_2 do not polarize [30]. The size of NP is also an essential factor that induces M1 polarization. Graphene oxide (GO) nanosheets with a larger surface area and are more oxidized, resulting in an induced release of inflammatory cytokines [53]. In contrast, smaller-sized Au-NPs exhibit a higher surface area per unit of weight is more effective in pushing cells to the M1 polarization state than bigger Au-NPs [51]. Considering all of these findings, the vital role of NPs is demonstrated their significance in macrophage polarization, ultimately influencing host immune

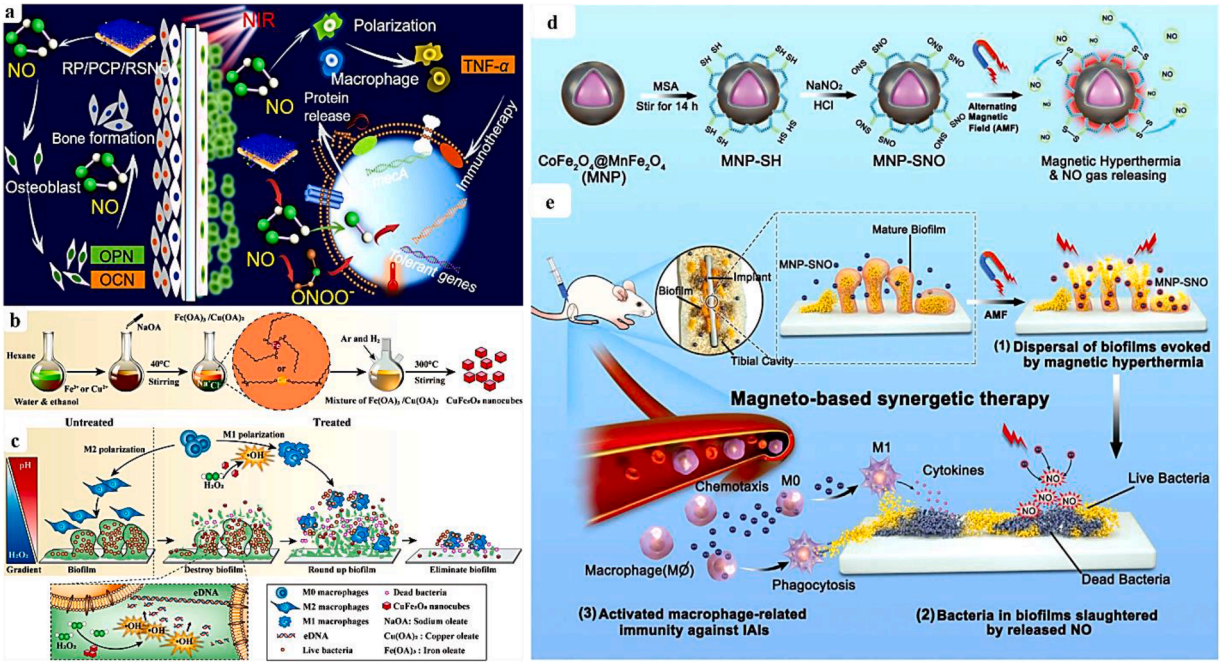

Fig. 3. (a) Schematic illustration showing the molecular mechanisms related to bone formation through M1 polarization of macrophage and eradication of methicillin-resistant *Staphylococcus aureus* (MRSA) biofilm through gene downregulation [55]. (b) Schematic diagram demonstrating the general synthesis approach and (c) the proposed anti-biofilm and immunomodulatory mechanisms of $CuFe_5O_8$ NCs [56]. (d) Schematic illustration highlighting nitrosated mercaptosuccinic acid (MNP-SNOs) synthesis and it's *in vivo* magneto-based synergetic therapy. (e) Schematic illustration of the ligand exchange and nitrosation procedures of magnetic nanoparticles ($CoFe_2O_4$@$MnFe_2O_4$) and the concurrent magnetic hyperthermia/NO gas production under the applied alternating magnetic field (AMF). Schematic illustration demonstrating implant-infected rat tibia undergoing treatments using MNP-SNOs under AMF: (1) fragmentization of compacted biofilms under magnetic hyperthermia through MNP-SNOs, and (2) release of NO abundantly from MNP-SNOs in a hyperthermal environment leads to death of sessile bacteria within biofilms. The MNP-SNOs upregulated levels of chemokines and immune responses to guide the macrophages toward the infection and trigger M1 polarization. (3) The growth of the surviving bacteria was further inhibited due to phagocytosis and cytokine secretion of M1 macrophages [57].

system.

2.3. Phagocytic cells

Macrophages and dendritic cells are phagocytic cells that use phagocytosis to remove pathogens and cell debris. They trigger the secretion of cytokines, causing an inflammatory response, and influence adaptive immunity by delivering antigens to lymphocytes *via* the TLR signaling pathway. Dendritic cells and macrophages are quick to ingest NPs. The uptake of NPs and their fate inside cellular compartments depend on their interaction with the phagocytic cells, which eventually correlates with the adaptive immune responses. Several reports indicated that metal-based NPs (magnetic NPs and NP-based PET agents) have been used to image macrophages and cell death in various bacterial diseases [54]. In addition, earlier studies have reported the theranostic effects of different NPs-mediated (Fig. 3) carriers over macrophages that effectively augments biofilm eradication through various molecular mechanism in the presence of external or internal stimuli [55–57].

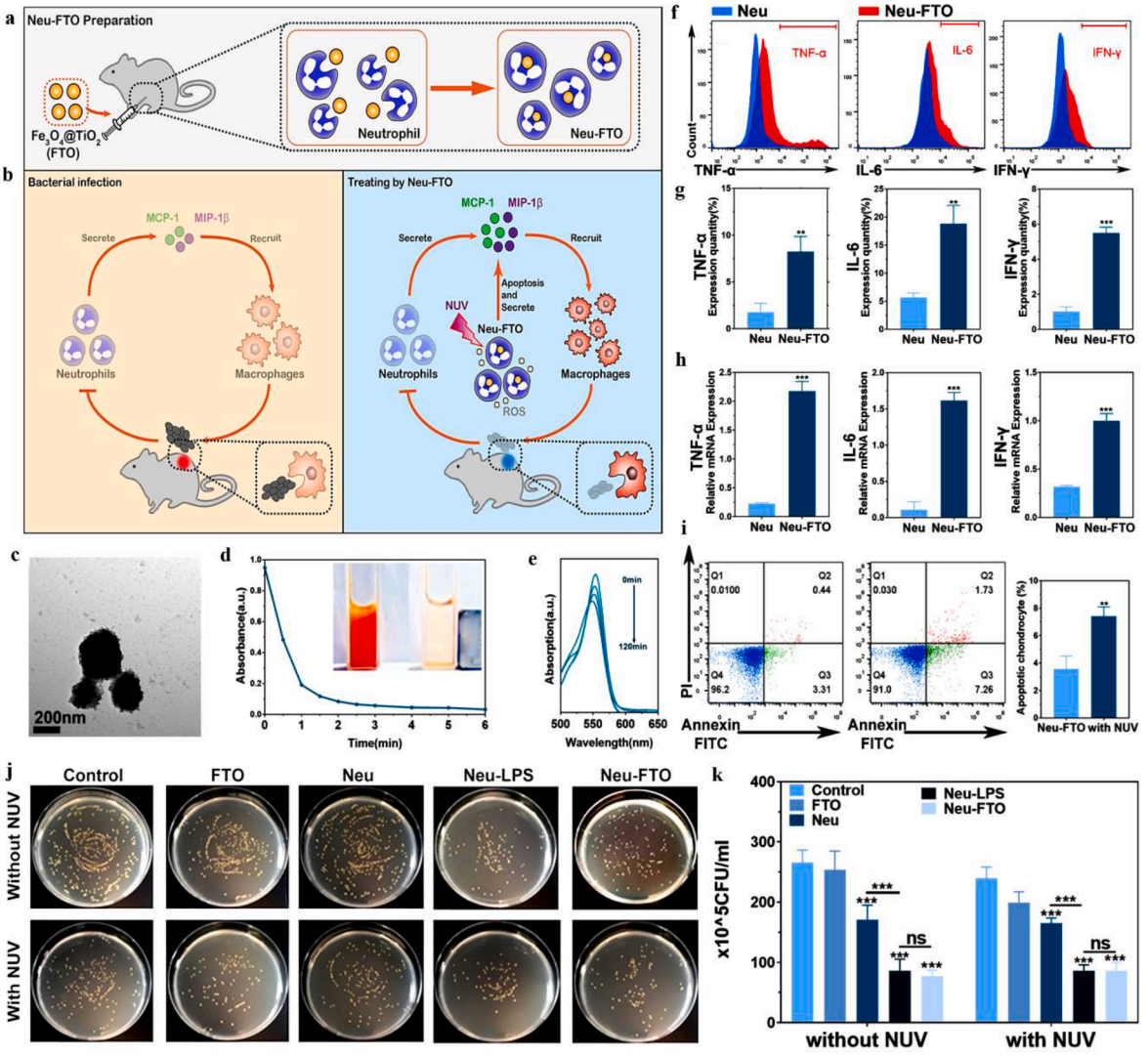

Fig. 4. (a) Schematic representation of process involved in the fabrication of neutrophil-conjugated Fe_3O_4@TiO_2 nanoparticulate system. (b) Illsutration desricbing the application of Neu-FTOs *via* local and systemic injection. (c) Morphological (TEM) findings of Fe_3O_4@TiO_2. (d) Magnetic property analysis of FTO in the presence of magnetic field and UV–Vis spectroscopy. (e) Photodegradation of RhB in the presence of catalysts. (f) Flow cytometry assay, (g) quantification, and (h) quantitative RT-PCR of TNF-α, IL-6, and IFN-γ expression. The data are presented as the mean ± s.e.m. (n =3). **p < 0.002, ***p < 0.001. (i) Flow cytometry assay and quantification of Neu-FTO apoptosis with or without NUV irradiation. The data are presented as the mean ± s.d. (n = 3). **p < 0.002, ***p < 0.001. (j) Photo- and (k) quantitative analyses of the bacterial colonies of MRSA incubated with PBS, FTO, neutrophils (Neu), Neu-LPS, and Neu-FTOs with or without near-ultraviolet (NUV) irradiation. The data are presented as the mean ± s.d. (n = 3). *p < 0.033, **p < 0.002, ***p < 0.001 [71].

2.4. Neutrophils

Polymorphonuclear neutrophils (PMNs) are the most free-circulating leukocytes and the first responder to tissue injury or site of infection. PMNs migrate to inflammatory sites to produce pro-inflammatory mediators and enhance the chemotaxis movement of monocytes-macrophages and lymphocytes. Au-NPs get entrapped in neutrophil extracellular traps (NETs), consisting of DNA and a range of antibacterial proteins [58]. The activating DNA receptors TLR9 and NETs trigger an immune response that aids immune cells recruited to develop an acquired immune response to inflammation. Depending on the location, timing, and dosage, NETs can combat the infection [59]. However, further investigation is required to determine the physiological roles of NETs generated by NPs. Vascular inflammation can be prevented by NPs mediated drug delivery to inflammatory neutrophils [60]. Thus, targeting active neutrophils by potential NP-based therapeutic strategy can provide a pathway for treating inflammatory diseases.

2.5. Mast cells

Mast cells are tissue-resident immune cells with a significant role in fibrosis and inflammation, pathogen clearance, angiogenesis, and immunoregulation. In case of allergy and anaphylaxis, mast cells get activated and release heparin and histamine, which causes vasodilation and recruit neutrophils and macrophages. TiO_2-NPs exhibit a dose-dependent increase in histamine secretion and cytosolic Ca^{2+} in mast cells [61]. The entry of NPs inside the body triggers histamine release without prior allergen sensitization, causing an aberrant inflammatory disorder. Mast cell granules enhance adaptive immunity when secreted at infection or vaccine delivery sites. Thus, NPs constituting mast cell granules are utilized to boost immunity during vaccination [62]. The metal-based NPs possess the potential to build this effective immunization. However, Nanomaterials as drug delivery vehicles provide significant potential as an effective method of modifying the biological activities of the mast cell.

2.6. T-cells

Several metallic NPs induce T-cell responses or homeostasis, thereby triggering the adaptive immune systems. TiO_2-NPs stimulate the release of inflammatory cytokines and increase dendritic cell maturation, expression of co-stimulatory molecules, activation, and proliferation of T-cells [63]. Cadmium confined inside fullerene cage NPs polarizes cytokine balances towards Th1 cytokines by decreasing Th2 cytokines (IL-6, IL-5, and IL-4) and increasing Th1 cytokines (TNF, IFN and IL-2) production [64]. AuNPs (10 nm) inhibited LPS-induced IL-12 p70 production by DC and promoted Th2 polarization, whereas AuNPs (50 nm) increased Th17 polarization [65]. Moreover, the modulation of Th1 or Th2 responses was generated by APC maturation and antigen absorption. The size of antigen-conjugated NPs determines whether they produce Th2 or Th1 immune responses [66]. Therefore, size of NPs can play an essential role in vaccine development depending on the need to trigger a response from the specific immune cell. The size of the NPs used for immunization impacts the type-1 or type-2 cytokine balance after vaccination. Other physiochemical features of NP, such as charge or chemical stability, have yet to be thoroughly investigated in relation to T-cell polarization.

2.7. B-cells

Upon antigen binding with the B-cell receptor, the antigen gets engulfed, digested, and presented on the surface with the MHC II complex for recognition *via* antigen-specific T helper cells. Upon receiving a signal from T-helper cells, B-cells are differentiated into antibody-secreting B cells. Antigen nanostructure boosts the response to B-cell antibodies [67]. Potential vaccination options for the generation of humoral immunity include calcium phosphate (CaP) NPs covered with antigens made of proteins [68]. Unless B-cells were covered with the antigen, NPs did not trigger them. Antigen-specific immunological processes, such as antibody production and T-cell responses, are harmed by FeO-NPs (as shown in Fig. 4) [69]. The impact of different metal-based NPs on B-cell activities should be further investigated, aiming at the humoral immune responses. In another study, tang et al. reported the potential role of AgB nanodots as potential antibacterial agent against methicillin-resistant *Staphylococcus aureus* (MRSA). AgB nanodots exhibited significant antibacterial actions through photo-thermal/dynamic therapeutic effects, and Ag^+ ion sterilization, both *in vitro* and *in vivo*. AgB nanodots significantly augmented the immune responses in the treated animals by upregulating the level of stress-mediated responses, including temperature spikes or excess ROS production. This lead to the stimulations of antibacterial effects of macrophages, dendritic cells, T-cells, and B-cells [70]. On the other hand, researchers developed neutrophils (Neu)-conjugated Fe_3O_4-TiO_2 (photocatalytic) NPs and demonstrated its potential antibacterial effects against MRSA. The mechanism illustrated in Fig. 4 reveals that the Neu-conjugated NPs demonstrated upregulation of ROS level through photocatalysis and promoted neutrophil apoptosis, leading to improved relocation of macrophages and activation of immune response cascades [71].

3. Physiological factors influencing NP-based strategies against MDR bacteria

Tremendous innovation in nanotechnology in recent years shows a promising future for developing antibiotic therapies as prospective medications against MDR bacteria. Antifouling surface properties of NPs provide an antibacterial effect and hinder bacterial adhesion and biofilm formation [72]. Additionally, such properties of NPs can be further achieved either by introducing antimicrobial NPs at the site of infection or antibiotics *via* nanocarriers. Herein we have discussed the factors influencing nano-systems against MDR infections.

3.1. Size and shape

The amount of NPs that have the potential to coat the cell's surface or the degree to which they penetrate the bacterial cell wall is determined by their average diameter when they are in contact with bacterial surfaces. NPs (as small as 50 nm in diameter) can target the DNA by breaking through the cell wall of bacteria. Ag-NPs with a diameter of 10 nm can penetrate bacteria and exert antimicrobial action [73] (as shown in Fig. 5) and have been reported to suppress the growth of *Bacillus subtilis* [74]. Conjugates of Au-NP: levofloxacin (27.2 nm diameter) showed higher potency against *Pseudomonas aeruginosa* (1.94-times), *Escherichia coli (*2.89-*),* and *Staphylococcus aureus* (1.46-times) than levofloxacin as a single agent [75]. The size of NPs proportionally enhances their intracellular entry and, therefore, increases their efficacy. For example, AuNP (45 nm) gets endocytosed *via* clathrin-mediated endocytosis, whereas AuNP (13 nm) gets phagocytosed entirely [76]. Besides the evident role of the size of NPs, how their shape plays a role remains understudied. The evaluation of various morphologies of silver NPs against *E. coli* and *S. aureus* for antimicrobial activity was found independent of the configuration of the AgNPs [77], indicating that the shape of NPs does not appear to play a severe influence in anti-microbial action as the morphology of AuNP upon interaction with NPs and plasma proteins plays a pivotal role in the anti-microbial activity. AuNP (diameter 25 nm and surface area 179.5 m^2g^{-1}) exhibited more potent fungicidal activity than gold polyhedral NPs (diameter 30 nm and surface area 150.5 $m^2\ g^{-1}$) for anti-microbial activity [78,79]. AgNPs (12 nm in diameter) of varied diameters kill *E. coli* owing to their anti-microbial effect [80]. Moreover, AgNPs exhibit antibacterial activity with a range of 1–100 nm efficiency against *V. cholerae, E. coli, S. typhus,* and *P. aeruginosa* [73]. AgNP with surfactants or polymers of size 26 nm exhibited antimicrobial properties against the bacterial strains isolated from clinical samples [81]. FeNPs synthesized from *Thymus valgaris* (40 nm diameter and spherical shape) also show antimicrobial activity against *E. coli, B. subtilis,* and *S. aureus* [82]. In summary, these studies reflected the size and shape of NPs don't play a deciding factor in antibacterial potency; therefore, other physical characteristics of NPs must be evaluated to improve their antibacterial efficacy.

3.2. Zeta potential

The zeta potential is an essential characteristic that aids in the interaction of NPs with the cell surfaces of bacteria [83]. It decides whether NPs can be used as drug delivery carriers for enhancing bacterial permeability to cause antibacterial activity. Zeta potential influences the pharmacokinetic behavior of NPs since pH variations modify the charge of the NPs. It is influential in determining the stability of colloidal NPs compositions in the 30 mV range [84]. A recent study showed that the LPS in the plasma membrane of gram-negative bacteria produces a negative charge on the cell surface that causes electrostatic attraction between the cells and the NPs, leading to a form NPs cluster on the cell surface rather than entering it [85]. Moreover, by inhibiting hydrophilic molecules from penetrating the outer surface membrane, LPS functions as a selective barrier [86]. However, the degree of attraction or repulsion between NPs and the bacterial cell surface is determined by the zeta potential, which makes it a determining factor as an antibacterial agent [87].

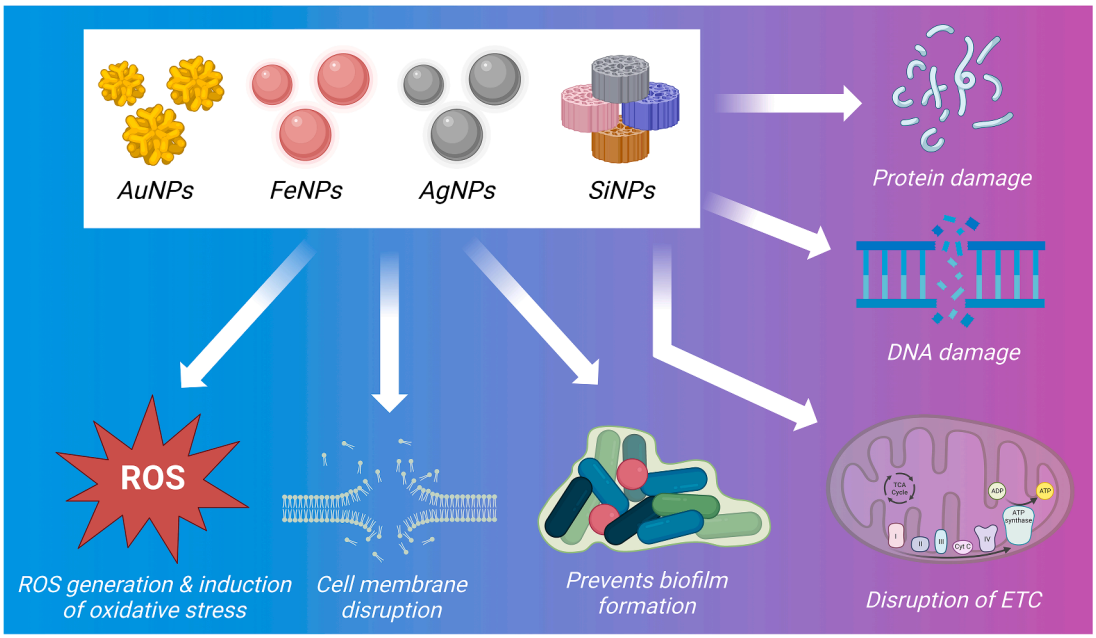

Fig. 5. A graphical model provides an understanding of the therapeutic mechanism of NMs for anti-microbial activity.

3.3. Optical properties

Surface Plasmon Resonance (SPR) is an optical property of NPs that creates an oscillation of conductive electrons which resonate on the metal surface upon activation by a specific wavelength of light. There has been much concern in biological research on the phenomena and occurrences of SPR in nanomaterials [88–90]. This optical characteristic is of great interest because it is tunable in altering the shape and size of the NPs for varied SPR phenomena. Au-NPs (diameter 70 nm) scatter light of the green spectrum and transmit light of the orange spectrum (max 530 nm). When Au-NPs are delivered, the absorption band of Au-Ag alloy NPs shifts towards longer wavelengths ("*bathochromic shift*") [91]. The SPR of the biosynthesized Ag-NPs (average diameter range = 400–500 nm) exhibits antibacterial activity against the MDR strain of *P. aeruginosa* [92]. Ag-NPs show *localized surface plasmon resonance* (LSPR, which is an interaction of light with a nanostructure that leads to a collective resonance of the conduction electrons in the metal [93]) and an efficient antibacterial effect of photodynamic therapy (PDT) compared to the Au-NPs. The physical characteristics of NPs, such as material type, size, shape, and microenvironment, determine the magnitude and resonance frequency of the LSPR effect [94]. However, photodynamic inactivation (PDI) has been widely explored with specific photosensitizers (PS) to target microorganisms [95]. To establish NP-LSPR-PS interaction, LSPR frequency and the absorption spectrum of PS must overlap; therefore, PS perceives field enhancement close to the NP surface, and a facile PS molecule excitation can be prompted [96]. Interestingly, spherical-shaped Ag-NPs show an LSPR peak in the blue region of the electromagnetic spectrum, and since some PSs (porphyrins and riboflavin) can be excited using blue light, singlet oxygen ($^1O_2$) generation by PSs could be enhanced by LSPR of Ag-NPs [97]. With such surface photochemical tools available to a chemical biologist, help to devise other *in-vivo* and *in-vitro* applications, such as improving the azobenzene physiological stability in photoswitches [98–101]. Various studies implicating the tandem use of the LSPR effect with PDI for Au-NPs conjugates with different PSs cited in the literature [102–104]. Exclusive to the antimicrobial effect, a profound reduction of *Candida albicans* biofilm was observed with AuNP-methylene blue conjugate using PDI, while other reports indicated the photodynamic treatment of cutaneous *C. albicans* infections [103] or Crohn's disease-associated *E. coli* [104] using Au-NPs. Au-NPs and Ag-NP with phthalocyanine-ε-polylysine conjugates showed effective PDI against *Staphylococcus aureus,* while silver conjugates were comparatively found more effective than gold nanostructures in this study [105]. The superior effectivity of silver over gold nanoparticles can be understood because LSPR can obtain a higher electromagnetic field enhancement in silver than in gold NPs [106,107]. Therefore, it made evident that LSPR enhances the photodynamic inactivation (PDI) of the bacteria. The interaction of LSPR with Ag-NPs upon functionalizing with riboflavin (Rb) through coated pectin (p-AgNP) mediated PDI against *Streptococcus mutans* and *E. coli,* showed enhanced riboflavin PDT on *S. mutans* but not on *E. coli* attributed with the lower uptake of Rb by *E. coli*. The PDI for gram-positive bacteria exhibits higher antibacterial effectivity as monotherapy and when coupled with AgNP. Rb-mediated PDI reduced viable cells by 77.5 % but the association of p-AgNP to Rb-mediated PDI reduced bacterial load by up to 99.2 % [108]. All the experimental data indicated that the efficacy of NPs is substantially conditional on their optical properties of NPs, which are eventually correlated with their size and shape, and also modification of NPs sometimes insists on manipulating their optical properties to enhance the anti-microbial activity. Therefore, it is important to focus on the optical characteristics, besides the physiochemical characteristics to rationalize the application of NPs to develop as an antibacterial effective.

3.4. Biocompatibility

Since most NPs prepared synthetic, their *in-vivo* toxicity can be manipulated to a minimum level, especially those NPs that include an antibiotic in the formulation that interfere with the antibiotic's mechanism or metabolism. However, the rational blending of specific polymers with antibiotics to mitigate the antibiotic's toxicity profile makes these nano-medicines safer. Vancomycin inhibits the formation of peptide crosslinking with peptidoglycan (PG) by binding to terminal D-Ala-D-Ala-residues in gram-positive bacterial cell-wall [109]. In vancomycin-resistant bacteria, the D-Ala-D-Ala-motif is transformed into D-Ala-D-Ser (VanB type resistance: lower-level enterococcal resistance) or D-Ala-D-Lactate (VanA type resistance: enterococcal resistance to vancomycin and teicoplanin) [110]. The transposable DNA genome contains the genes required for VanA-type resistance [111]. The conjugated polymer based on chitosan NPs provided reasonable biocompatibility, which reduced the conjugate's toxicity. NPs of poly(lactide-co-glycolide) (PLGA) entrapping gentamycin, with diameters ranging from 241 to 358 nm, showed controlled release and effectivity against *P. aeruginosa* [112]. PLGA, like chitosan, is clinically approved and biocompatible, allowing for the *in-vivo* application of AMR [112]. Studies on accessing the toxicity versus biocompatibility of NPs, remain contradictory; therefore, thorough experimentation is required. However, seeing the considerable success of NPs applicability in recent years in various fields indeed show a potential application; consequently, it is crucial to find a universally agreed-upon, bias-free toxicological model by focusing on both *in-vitro* as well as *in-vivo* investigations for clinical approval of any NPs as an antibacterial agent.

3.5. Surface topology

Besides impacting the aerodynamics of insect flights at the macroscale, surface topology plays a decisive role in altering the microenvironment of the biofilm formation [113–116]. The antibacterial mechanisms of nano-structured or patterned surfaces are highly exploited by examining the particular effects, such as distribution density and nano-pillared shape. An increased number of nanopillars per unit surface is advantageous to enhance a more significant adhesion area and fatal impact [117]. A lower density linked with using sharp nano-pillars exhibits antibacterial activity against *P. aeruginosa* [118,119]. The nano-pillars with a high aspect ratio possess a higher antimicrobial efficacy [120]. Interestingly, it is observed that bioinspired antifouling surfaces have been designed using lithography and self-assembly methods [121–123]. A variety of synthetic compounds produced for this technique *via* utilizing

the antifouling properties prevent the adhesion of bacteria on the surface of nanomaterials, thereby minimizing the biofilm formation [8,121–123]. Experiments are still needed to investigate how the topology affects the transport of NPs in macromolecular networks, which remains elusive.

3.6. Steric repulsion

Surface integration by long-chain polymers prevents bacterial cell attachment due to hydrophobic repulsion and surface steric hindrances. For instance, polyethylene glycol (PEG) and polyethylene oxide (PEO) are two polyethers polymers with the same repeating unit but different molecular weights commonly used for this purpose. Since they have low surface energy and form weak interactions with proteins, they are potentially ideal materials to prepare antifouling surfaces [124]. The zwitterionic polymer contains equal parts of anionic (carboxylate, sulfonate, and phosphate) and cationic (protonated amino, quaternary ammonium, pyridine) groups, display antifouling properties because of their low energy and structure [125,126]. Chemically, these zwitterionic polymers are stable, water-repellent, and restrict bacterial cell attachment to the material surfaces [127,128]. Zwitterionic polymers are electrospun from low-concentration, low-viscosity precursor solutions [129,130]. The creation of vascular grafts employing polyurethane matrices is one of the most notable applications [131]. Though there are few polymeric compounds reported for their antifouling effects, which are successfully used to prevent bacterial entry into the host, further investigations are needed to understand their

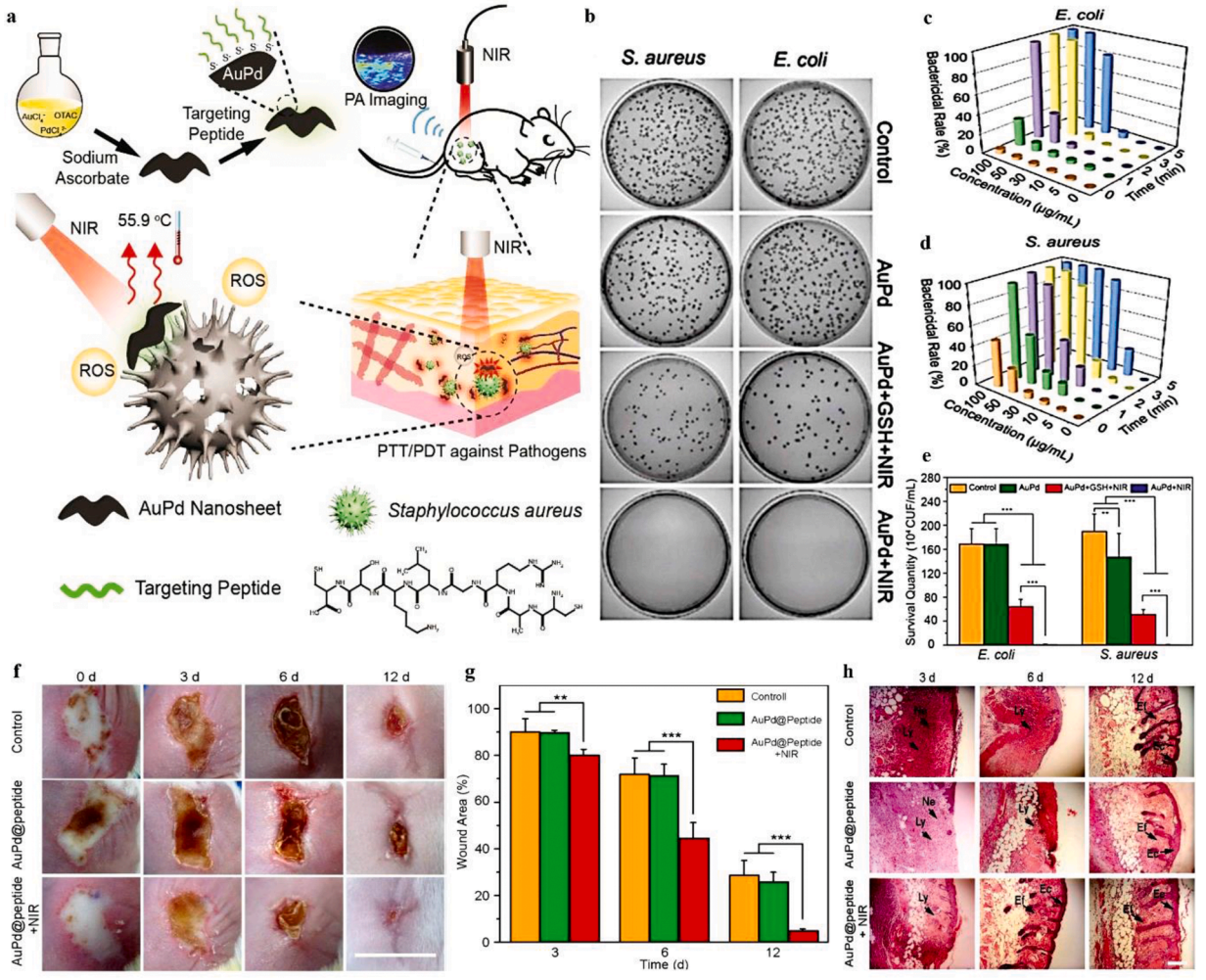

Fig. 6. (a) Schematic description of synthesis approach and alteration of gold-palladium (AuPd) nanosheets, and its potential antibacterial activities *in-vivo* against *S. aureus* mediated subcutaneous abscesses. (b) Plate count method in four groups for *E. coli* and *S. aureus* (control, AuPd, AuPd+GSH+NIR, AuPd+NIR; concentrations of GSH and AuPd are 0.5 mg/mL and 50 μg/mL respectively). (c) Time-and concentration-dependent antibacterial activity against *E. coli* (d) Time-and concentration-dependent antibacterial activity against *S. aureus*. (e) The data presented for figure b as n=6, **P<0.01, ***P <0.001. (f) Images of *in-vivo* findings of *S. aureus* infected subcutaneous abscess. (g) Corresponding statistics for wounds mentioned in figure f (**p < 0.01; ***p < 0.001). (h) H&E staining of skin tissues of *S. aureus*-infected wounds of mice (Ly: lymphocyte; Ne: neutrophil; Ec: epithelial cells; Ef: elongated fibroblasts) [132].

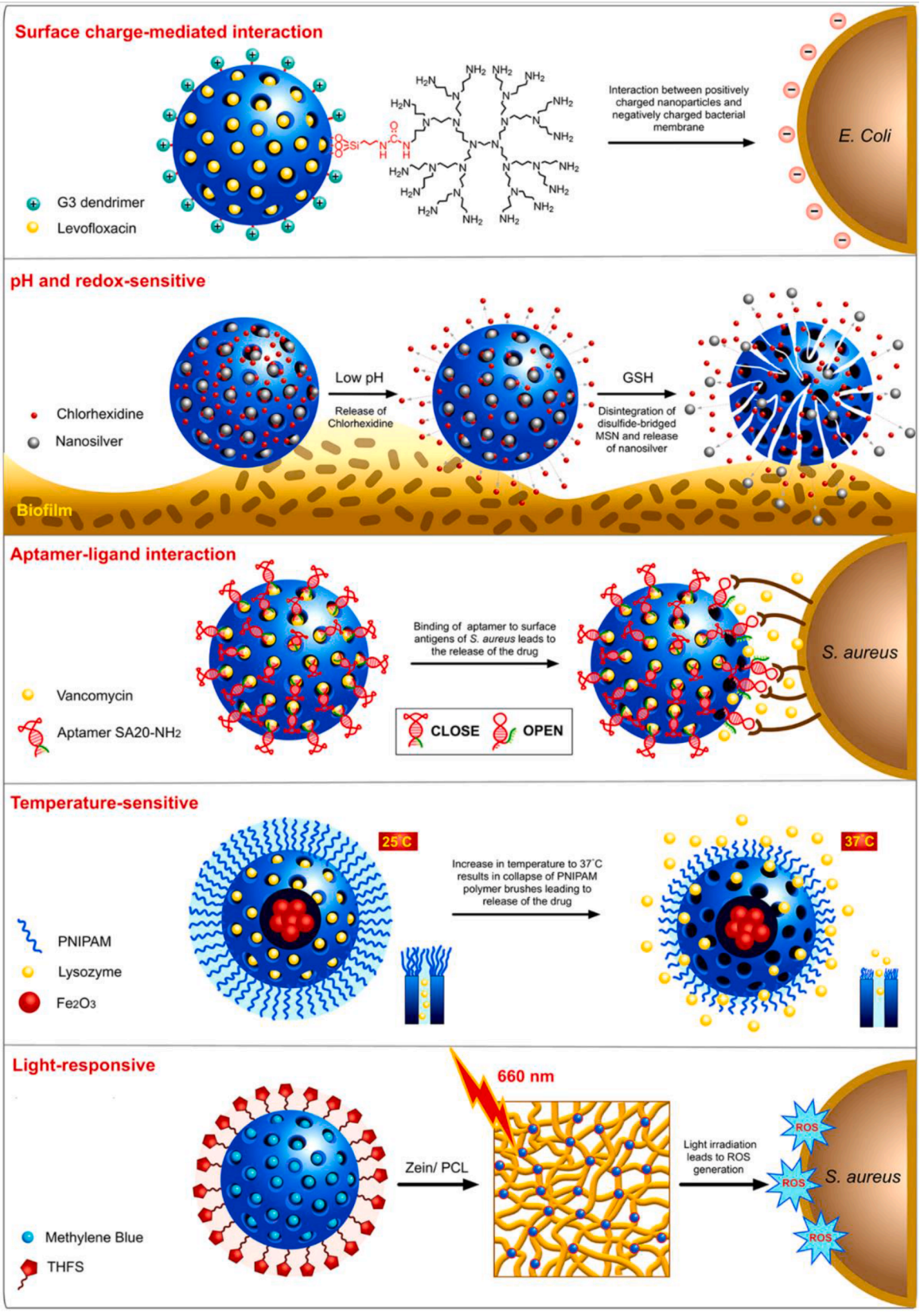

Fig. 7. Various strategies are involved in the targeted delivery of antimicrobial agents based on mesoporous silica nanoparticles [150].

working principle before finding their clinical applications.

4. Synthesis of nanotheranostics used for anti-bacterial activity

Various preparations were devised for NPs which inherited antimicrobial properties (as shown in Fig. 6). Some common physical techniques, which require high temperatures, were found time-consuming, sustain high thermal load to the equipment, and are less energy cost-efficient. Therefore, there is a trend of using chemical treatments, where chemical reduction is the most preferred method for producing organic and inorganic NPs. In chemical reduction, mainly three reaction components are involved (a) precursor, (b) reductant, and (c) stabilizer. However, there are applied physiochemical methods which interested material chemists in recent years for preparing antimicrobial NPs, such as nucleation, microemulsion, photo-induced reduction, and synthetic electrochemical methods [132]. Interestingly, chemical synthesis produces comparatively higher yields than the yields from physical methods, but due to low-to-none solvent usage in physical methods, these processes are usually devoid of solvent impurity and possesses uniformity of NPs distribution. Further, the synthesized gold-palladium (AuPd) nanosheets exhibited potential antibacterial activities *in-vivo* against *S. aureus* mediated subcutaneous abscesses [132]. However, biologically-derived NPs show comparatively higher stability over chemically synthesized ones, and therefore, organisms with a biosynthetic ability (such as bacteria, fungi, and plants) have gained significant attention in recent years [133].

4.1. Silicon NMs

Non-metallic Si-NPs are usually prepared with Stober's and microemulsion methods, resulting in monodispersed silica particles in the sub-micrometer range [134]. Commonly, tetraethyl orthosilicate (TEOS) is used as a silica precursor, which initially gets hydrolysis (in the presence of ethanol and ammonium hydroxide), and undergo polycondensation to form non-porous silica particles (diameters smaller than 200 nm) (Fig. 7). Furthermore, Rao and his colleagues improvise to develop a sequential method, where they achieved various particle size of monodisperse and uniform-size silica NPs 20–460 nm using ultrasonication by sol–gel process [135]. Other low-cost silica precursors, such as sodium silicate solution, have been employed in addition to TEOS [136,137]. The surface of these NPs are rich in silanol groups, which is used to tether with surface functionalizing organosilanes, such as (3-aminopropyl) triethoxysilane (APTES) and (3-mercaptopropyl) trimethoxysilane (MPTMS) [138]. Other alternative methods for Si-NPs preparation consist of microemulsion [138–140], spray drying [141], low-temperature vapor-phase hydrolysis [142], and chemical precipitation [143].

Non-porous Si-NPs, mesoporous Si-NPs (MSN), hollow mesoporous Si-NPs (HMSN), and core-shell SiNPs, characterized by TEM (Transmission Electron Microscope) and SEM (Scattering Electron Microscope) [144,145], are the most prevalent morphologies of Si-NPs synthesized utilizing the above-mentioned methods. The physicochemical properties of NPs, such as size, shape, and porosity, are essential in delivering payloads to the target site. Si-NPs are typically produced in sizes ranging from 10 to 500 nm [144,145]. Particle size is usually adjusted by changing the reaction conditions such as ammonia/sodium hydroxide concentration, stirring speed, or TEOS addition rate [144,145].

Si-NPs, notably MSN, have been extensively used as drug delivery agents. For example, triclosan (Irgasan), an FDA-approved antibacterial, was covalently attached to the surface of Si-NPs using a 3-(triethoxysilyl) propyl isocyanate (TESPC) coupling agent, which improves drug loading efficacy [146]. In another investigation, vancomycin conjugated with amine-modified, FITC-loaded MSN for selectively targeting gram-positive bacteria [147]. Another nano-antibiotic system comprising of MSN loaded with levofloxacin (LEVO) and surface functionalized with positively-charged *N*-(2-aminoethyl)-3-aminopropyltrimethoxysilane (DAMO) for selectively targeting negatively-charged bacterial membranes and biofilms [148]. Interestingly, researchers are exploring antibiotics: Si-NPs conjugate to target antibiotic resistance strains [149]. In addition, researchers have reported numerous potential approaches for the targeted delivery of various antimicrobial agents in antibacterial therapy using mesoporous silica nanoparticles as carrier (Fig. 7) [150].

4.2. Chitin nanofibril

Chitosan is the second most naturally abundant biopolymer, hydrophilic in nature, with reasonable biocompatibility and mechanical structural qualities. With such materialistic properties, chitosan and its derived versions provide a wide range of applications, especially in the biomedical industry [151]. The spray-drying technique is one of the typical processes for producing chitin nanofibril (CN) with an average length of 250 nm. Infrared (IR) spectroscopy, thermogravimetry, X-diffraction spectrometry, and electron microscopy (for example, TEM, SEM) are commonly used to evaluate the synthesis of the CN qualitatively [152].

Coltelli's research group has shown CN extraction and deacetylation from crustaceans' shells (dCN) and their potential applications as antimicrobial agents in carboxymethyl cellulose (CMC) films, demonstrating the superior antimicrobial efficiency of dCN/CMC films over CN/CMC films. This study also provides the significance of CN surface chemistry in developing advanced therapeutic applications [153]. Another top-down method of producing CN was developed by Ifuku *et al.* The nanofibers of uniform width of 10–20 nm were characterized using FE-SEM (Field Emission Scanning Electron Microscope) [154]. However, additional studies are required to devise a proficient extraction and isolation of CN to evaluate their therapeutic efficacy.

4.3. Polyhydroxyalkonates

The synthesis of polyhydroxyalkonates (PHAs, also known as PHACOS) containing thioester groups on the side chain makes them

accessible for chemical functionalization and, therefore, their potential application as biomedical materials [155]. The PHACOS produced by wild-type *Pseudomonas putida* KT_{2442}FadB and its derived strain (fadB gene mutated), characterized at the molecular level with the help of nuclear magnetic resonance (NMR) and gas chromatography-mass spectrometry (GCMS–) [155].

PHAs showed a broad spectrum of activities, including antifungal, antibacterial, anti-inflammatory, antibiofilm, and virucidal effects, depending on the conjugated intrinsic bioactivity. One of the applications where PHAs were found useful is improving antibiotic delivery, such as the growth of *P. aeruginosa* and *C. albicans* was inhibited by the drug-releasing mechanism of PHA NPs. Therefore, the intrinsic antimicrobial properties of PHAs should be considered when conjugation with antimicrobial agents for biomedical applications.

4.4. TiO_2 nanopillars

TiO_2 nanopillars are known to be generated on grade 5 titanium alloy using a thermal oxidation process (Ti-6Al-4 V) to construct bio-inspired antibacterial nano-topography surfaces [156]. The surface of the nanopillar NW-850–5 was oxidized at 850 °C for 5 minutes, resulting in a nano-topography that closely resembled the nano-protrusions observed on dragonfly wings. The nanopillars were made of TiO_2 and were mostly made of rutile TiO_2 [157]. The resultant oxide surface changed from nanopillar forms to nanospikes by adjusting the acetone vapor concentration within the tube furnace. The topology of the nanospikes may be modified from column-shaped structures to extremely thin wires with widths in the area of 20 nm by adjusting the flow rate through the acetone bubbler and thereby increasing the quantity of acetone vapor in the tube furnace. The SEM and XRD images characterize the synthesized nanospikes after removing the outer carbon shell.

In the era of nanotheranostics, the intrinsic antibacterial TiO2 nanopillar activity can find a wide range of material applications that exclusively address antibiotic resistance. Such as the cell wall composition of *Pichia pastoris* altered in the presence of TiO_2 in response to ROS effects [158]. *E. coli* (gram-negative) cell walls comprised of LPS have been observed to be susceptible to TiO2 peroxidation. Some studies suggested TiO2 NPs more antibacterial towards gram-positive bacteria [159], while others suggested more toward gram-negative bacteria [160].

4.5. PMMA functionalized chitosan nanoparticles

PMMA-functionalized chitosan nanoparticles were synthesized *via* mini-emulsion polymerization [161]. In this synthetic method, sequential addition of reagents is advised, where methyl methacrylate (MMA) monomer containing 2,2′ -Azobisisobutyronitrile (AIBN) and hexadecane were stirred with CS solution for an hour and then sonicated in ice-bath (2 mins) [161]. Thereafter, the solution temperature is raised to 80 °C for 2 hours, and a sustainable polymerization occurs in the reaction media [161]. The effects of polymerization time and AIBN concentration on % conversion were investigated. At last, the freshly prepared PMMA-functionalized chitosan nanoparticleswas purified by iterative centrifugation until the conductivity of the supernatant came close to the deionized water [161]. Dynamic light scattering (DLS) is used to measure the average size, size distribution, and zeta potential of PMMA-CS [161]. The Dh values were inversely proportional to the CS concentrations, i.e., the Dh decreased from 450 nm to 380 nm when the CS increased from 0.25% to 1% [161]. TEM was used to study the morphological characteristics of PMMA-functionalized chitosan nanoparticles, where spherical particles with an average size and polydispersity index were found 338 nm and 1.04, respectively [161]. Staining with 2% phosphotungstic acid, the core-shell morphology of the prepared PMMA-functionalized chitosan nanoparticles was revealed. The positive charge on the PMMA-functionalized chitosan nanoparticles surface was confirmed by measuring the zeta potential (+64 mV to +29 mV at pH 2–7) [161]. Suteewong's research showed a significant increase in the antibacterial activity of chitosan nanoparticles against *E. coli* and *S. aureus* upon PMMA functionalization derived from their inherent materialistic properties, such as repelling and contact-inhibition mechanisms [162]. Furthermore, these modifications showed lower cytotoxicity, demonstrating their futuristic application with high surface roughness and minimal cytotoxicity for biomaterial research.

4.6. Poly (2-N, N-dimethylaminoethylmethacrylate)

Poly (2-N, N-dimethylaminoethylmethacrylate) (PDMAEMA) is a water-soluble pH-sensitive cationic polymer. Its intrinsic cationic charge over tertiary amine groups enhances the PDMAEMA propensity to form nanoencapsulation material, therefore, can serve as a reasonable biomaterial for drug and gene delivery [163]. Free radical polymerization is a typical method for preparing PDMAEMA [164]. Purified 2-N, N-dimethylaminoethylmethacrylate (DMAEMA) monomer, and AIBN (an initiator) were mixed under an inert atmosphere in a heatring reactor for seven days to produce a solid polymer. A conventional method for preparing the PDMAEMA involves a solution of DMAEMA in toluene with initiator 2,2-azobis(2-methylbutyronitrile) (AMBN) [165]. In addition, dodecanethiol (C_{12}-SH) was utilized as an agent for chain transfer to control the molar mass of the polymer produced. To improve the degradability of PDMAEMA, initially, BDMO (5, 6-benzo-2-methylene-1,3-dioxepane) monomer and DMAEMA were mixed under an argon atmosphere, followed by the addition of PEO (free-radical azo-initiators) and PEG6000 (cytotoxicity reducers) and the reaction mixture heated for 24 hours [166], as shown in Fig.7. Followingly, the mixture was diluted with chloroform ($CHCl_3$) and precipitated in pentane. Due to the high number of ester bonds in the structure, the resulting PDMAEMA demonstrates enhanced degradable and water-soluble. Surface modification of PDMAEMA NPs provides target-oriented characteristics accompanied by some stimuli-sensitive response, influencing the biodistribution of NPs to modify the subsequent uptake routes of bacteria to prevent their entry into the host [166].

4.7. Cationic liposome

Cationic liposomes were synthesized by varying the lipid film hydration process [167] based on the lipids involved. To create lipid bilayers, lipids are dissolved in $CHCl_3$. The lipid's transition temperature regulates the fluidity of the lipid bilayer to shift the lipid's physical state from gel to liquid crystalline. The resultant clear lipid solution was evaporated under reduced pressure, yielding the lipid bilayer, which was kept at -81 °C for at least 24 hours to avoid phospholipid degradation. After 24 hours, the lipid bilayer was hydrated in two stages with 2 ml of an aqueous HEPES solution, producing multilamellar and polydisperse liposomes.

The hydrodynamic radius of cationic liposomes with an average size of around 100 nm is reasonable to perform as an intravenous drug nanocarrier [168]. Interestingly, the zeta potential of liposomes slightly depends on the amount of lipid added, and no change was observed with anionic liposomes when lipid content is increased. However, the zeta potential was found to decrease with lipid content at a constant proportion of cholesterol and cationic surfactant [168].

Though liposomal phospholipid bilayer passively fused with bacterial membranes, transferring a higher amount of direct drug delivery into the bacteria. To avoid rejection of the reticuloendothelial system (RES) during drug delivery, cationic liposomes are employed to improve the penetration into infectious biofilms [169]. However, the surface functionalization of liposomes is still challenging and therefore requires a rational choice of manufacturing target-specific, pH-sensitive liposomes to achieve the intended application. Therefore, developing liposomes that can penetrate the biofilms and minimize their bacterial growth in those micro-colonies remains understudied [169].

4.8. Cefquinome sulfate cationic proliposome

A solid-dispersion approach combined with effervescent hydration is typically used to synthesize Cefquinome sulfate cationic proliposome (CSCPs). To prepare the lipid solution, soybean phosphatidylcholine and cholesterol were dissolved in $CHCl_3$ and Tween 80 with continuous stirring, and later Cefquinome sulfate, octadecylamine, citric acid, and sodium bicarbonate were added [170]. Under reduced pressure, $CHCl_3$ is removed, and the reaction mixture is dried over 24 hours to produce drug-proliposomes, which were then hydrated to form CSCLs by adding sodium bicarbonate. CSCPs are small yellow particles that are hydrated to become white CSCLs [170].

SEM microscopy revealed CSCPs are uneven in form, with regular concave, convex surfaces and occasional lamellar features [170]. The average drug loading (4.04% $\pm$ 0.04%) and % entrapment efficacy (63.21% $\pm$ 0.12%) of liposomes were estimated using a C_{18}-reverse phase High Permonace Liquid Chromatorgy (integrated UV–vis detector (270 nm). The CSCLs average particle size is 201.5 nm, ranging from 50 to 1000 nm in size, with a zeta potential of 65.29 mV and a high polydispersity index [170]. Cefquinome sulfate is a broad-spectrum antibiotic that is equally potent against gram-negative and gram-positive bacteria and effective against the resistant strain of *S.aureus* [170]. However, the inhibitory effect of CSCL against *S. aureus* is more potent than Cefquinome sulfate, which requires further investigation of its antibacterial mechanism before its preclinical development.

4.9. Polymersomes

Polymersomes are self-assembled, block copolymer vesicles with extensively cross-linked, tunable membranes, usually produced from free radical polymerization [171]. The polymersomes maintain free radical polymerization of the hydrophobic butadiene, resulting in a semipermeable nano-shell. Cross-linked gigantic vesicles are persistent in $CHCl_3$, dried, and rehydrated without destroying the 9 nm thick membrane core. Surface elastic moduli and long-term wall tensions are consistent with significant tethering between close-packed neighbors: elasticity and mechanical stability of cross-link-diluted vesicles created by mixing the non-cross-linkable counterpart at different molar ratios. Won and co-workers [172], used polybutadiene in the cores of the vesicle membranes cross-linked by free radical polymerization in solution, with radicals created by an initiator ($K_2S_2O_8$) and a redox couple ($Na_2S_2O_5/FeSO_4{\cdot}7H_2O$). As previously reported, anionic polymerization was used to create block copolymers [172,173]. Vesicles occur spontaneously by hydration of either bulk copolymer or dried copolymer films generated by $CHCl_3$ evaporation. Bright-field pictures show giant, spherical, unilamellar polymersomes. Separate cryo-TEM images reveal that the hydrophobic core thickness is 9$\pm$1 nm. A vesicle SEM is made simply by vacuum-drying it without staining or fixing, indicating the vesicle's long axis to be 10 μm [171].

Due to low antibiotic bioavailability and commonly exhibiting AMR, the facultative *Burkholderia pseudomallei* is a microorganism challenging to target with typical antibiotics. However, Porges *et al.* used imaging flow cytometry (IFC), to demonstrate the co-localization of polymersome with intracellular *B. thailandensis*, which suppresses their proliferation upon the incorporation of antibiotic-loaded polymersomes by infected macrophages [174]. Furthermore, compared to free antibiotics or polymersome alone, polymersome-encapsulated metronidazole or doxycycline dramatically reduces the intracellular gram-negative anaerobe *Porphyromonas gingivalis*, which is associated with periodontal disease [175]. Being an excellent antibiotic carrier, advancements in polymersome designing and drug delivery optimization are the current focus to reach maximum antibacterial potential [176].

4.10. Polymeric micelles

Polymeric micelles (PM) are self-assembled nanostructured core-shell structures generated inside water by amphiphilic copolymer that retain hydrophobic moieties inside the core of micelles and hydrophilic bioactive molecules such as DNA or siRNA in the outside shell of PMs. PMs are typically 100 nm in size and are employed for the systemic administration of hydrophobic medicines. A solvent-

diffusion approach was used to create the rifampicin-loaded PMs [177]. Rifampicin (RIF) was dissolved in acetone by sonication, and the organic solution was then injected dropwise to an aqueous dispersion under magnetic stirring at room temperature overnight to ensure acetone evaporation using a programmed syringe infusion pump. Finally, the volume of the RIF-loaded micellar dispersion was adjusted and filtered. Filtered samples were kept in amber glass vials until usage.

UV/Vis spectrophotometry estimated the RIF concentration. TEM was used to examine drug-free and RIF-loaded PMs. DLS was used to measure the critical micellar concentration (CMC) in an aqueous solution, hydrodynamic diameter (D_h), and size distribution of PMs in the absence and presence of RIF. Drug-free dispersions initially had a narrow and uniform size distribution with a D_h of 77 nm, while RIF-loaded micelles are of D_h of ~107 nm [177].

Zhou *et al.* developed a copolymer of PEG-b-P3/4HB-b-PEI-b-FA (EHP-FA) and PEG-b-P3/4HB-b-EPL (EHE), which showed *in-vitro* as well as *in-vivo* antibacterial efficacy against *S. aureus* [178]. Another study demonstrated that PMs based on poly [5-(benzyloxy)-4-oxo-4H-pyran-2-yl] methyl acrylate/polyacrylic acid/chitosan (PBOPMA-PAA-Cs) containing suspended kojic acid groups with efficient antibacterial activity against gram-positive and gram-negative bacteria compared to gentamicin and ampicillin [179]. More such PHM are under investigation for their hemocompatibility, cytotoxicity, and gene silencing effectiveness, aiming for clinical applications.

4.11. Nanodiamonds

Nanodiamonds (NDs) are carbon-based biocompatible NMs that are promising candidates for targeted therapeutic applications and other biomedical applications such as bioimaging and implant coatings. Detonation techniques, laser-assisted synthesis, high-temperature high pressure (HTHP) high-energy ball milling of microcrystalline diamond, hydrothermal synthesis, chemical vapor deposition (CVD) synthesis, ion bombardment on graphite, carbide chlorination, and ultrasonic cavitation, are mainly used to synthesize NDs [180]. The surface of NDs is functionalized in various ways depending on the intended application. The explosion of carbon-containing explosives in an aerobic environment produces small NDs in the 2–10 nm range. The graphitized outer layer allows for surface group functionalization, such as partial surface oxidation [181] and the addition of glycan groups [182], resulting in a range of distinct surface functions that depend on pretreatment and processing.

DLS measurements of the NDs' particle sizes and surface charges were confirmed using zeta potential measurements. Fourier transform infrared spectroscopy (FTIR) was used to examine the functional groups on the ND surface. Furthermore, the ND morphology was studied using TEM imaging. NDs were found to prevent *E. coli* and *S. aureus* biofilm formation [183]. Furthermore, surface-functionalized NDs are far more effective in antimicrobial activities against gram-positive and gram-negative bacteria [183, 184].

5. Nanomaterials against AMR

The antimicrobial applications of biomaterials are centrally focused on diminishing the ramifications of biofouling and bacterial colonization with the added advantage of excluding the dependency on drugs that potentially induce bacterial resistance [185]. The inherent anti-microbial and anti-fouling characteristics of these NMs have been establishing pillars of success in the biomedical domain owing to the advancements against surgical complications and healthcare-linked infections, predominantly categorized into physical or mechanical, electrostatic, and chemical divisions. The urgent need for application-based utilization of polymeric NPs is associated with skin anomalies, particularly skin damage [185].

Skin, susceptible to infections, captivates bacterial infections, including *Pseudomonas, Corynebacterium, Micrococcus*, and *Streptococcus*, in disseminating the damage while further targeting internal organs and their surrounding tissues [186]. The interaction of NPs with bacterial cells causes alteration of unsaturated fatty acid composition in the cell membrane for alteration in membrane fluidity. *P. aeruginosa,* when exposed to NPs, alters the unsaturated fatty acid composition for changes in membrane fluidity to inhibit the entry of NPs into the cell [187]. Silicon NMs have exhibited biocompatibility both *in-vivo* and *in-vitro,* and its topology prevented bacterial colonization while being effective against *P. aeruginosa* and *S. aureus* without eliciting an inflammatory response when COS-7 fibroblast cells are placed in contact with the black silicon surface [150]. This topology can be implemented for anti-bacterial activity in implants and prosthetics. Black silicon used to develop a microfluidic device exhibited bactericidal activity *via* nano spikes and bacteria near operated under static and kinetically active conditions [188]. Hence, silica in the nanostructured form characteristic of nano protrusions having a high aspect ratio was shown to effectively combat *E. coli, S. aureus,* and *B. cereus*.

The change in the environment of the bacterial cell due to NPs triggers mutation and genome plasticity causing the evolution of AMR species to become persistent. NMs overshadow the elicitation of infections originating from percutaneous implants that foster the colonization of bacteria. These bacteria can either be intrinsic or swoop their way in from the external environment [189]. In case of severe infection where the wound penetrates to deeper sections underneath the epidermal layer, antimicrobials hinder the bacterial colony, originating from substitute grafts that cannot be replaced by keratinocytes [190]. Anti-fouling mediums aim to disrupt the adhesion forces and elicit repulsive interactions on microbial contact with the surface of our body. The active forces facilitating anti-microbial activity are physical or chemical, or electrostatic, whereas those facilitating antifouling activity are physical, steric, or electrostatic [191]. Biomaterials encompassing polymeric chains inhibit adsorption and possess intense hydrophobic structures that elicit conditions to hinder the linkage of foreign particles by enhancing repulsive forces while inducing electrostatic polarization [192, 193]. The proliferation of bacterial colonies manifests biofouling through non-tubular fibrous marks around the implant, pertaining to the need for antibiotic therapy. A layer of nano-structures in the form of sharklets encases the surface region possessing the potential to decelerate colonization without initiating resistance but retaining certain limitations owing to resilience and cost [193,194]. The

super-hydrophobicity caused due to emplacement of fibrous networks and roughness quotient arises from the electrospinning of super hydrophobic models characterized by small fiber diameters [195]. However, these biomaterials could not persist in their endurance post-implantation and are subject to biodegradation, biosorption, and bio-resorption. Bioactive characteristics were manifested in various sub-classes of sulfated polysaccharides from different seaweeds, including ulvan, galactan, and fucoidan. Ulvan is renowned for its antimicrobial and antifouling activity, impedance to viral pathogenesis in HSV-1 virus, and suppression of biofilm formation by exhibiting anti-cohesive properties of negative charges and disproportionate surface [195,196]. Hence, a closer insight into these biomaterials' antimicrobial and antifouling characteristics and their subsequent role in curbing post-surgical and skin related complications has been highlighted [197]. Fig. 8 illustrates the role and mechanisms of NMs in combatting anti-microbial infections. Table 1 discusses the clinical significance of NMs in fighting anti-microbial infections.

5.1. Cationic and hydrophobic nanomaterials

Nanomaterials possessing cationic-hydrophobic functionalizations presenting a reasonable antibacterials activity as cationic functionality assists in making ionic-ionic interaction with negatively charged bacterial membranes, while hydrophobic functionality alter the osmotic pressure leading to cytoplasmic leakage. [198,199]. The cationic polymers are intrinsic biocompatible materials dependent on the physicochemical properties of the materials with low immunogenicity and toxicity, requiring no additional cost [163,200–202]. These polymers' volumetric distribution and helical organization lead to the allocation of cationic and hydrophobic groups that potentially aggrandize anti-microbial activity in *Staphylococcus aureus* and *Enterococcus faecium*, wherein the pathogens possess the innate potential to absorb hydrophilic groups for cell death [203–209]. Anti-inflammation and anti-bacterial features are exhibited by another class of molecules, namely CN especially post *in-vitro* administration to human keratinocytes by counter-reversing the effects of pro-inflammatory cytokines such as TNF-α, IL-6, IL-1α, and IL-1β. However, the efficacy of CN is boosted by surface coating rather than bulk administration [210–212]. The role of PHAs integrated with sulfur groups, and thioester moieties (PHACOS) is associated with their antimicrobial activity. PHAs exhibit biocompatibility, biocidal activity, and bio-resorption from renewable sources for biomedical applications. Apart from acting as a substitute for petroleum-sourcing plastics, their thioester and alkyl groups also establish direct contact with microbes such as *S. aureus* to elicit biocidal activity [155,213–216].

PMMA is a biocompatible packaging material for medical implants in the bladder used to investigate antimicrobial activity in rat models. An intra-vesicular change in the levels of inflammatory cytokines and migratory inhibitory factor (MIF) was manifested post administration of PMMA coated ball, causing downregulation of IL-1β, IL-6, and TNF-α and reduced MIF for cytotoxic effect and effective functionalization of the implanted device [217]. The biomedical applications of PMMA are prevalent in orthopedic implants and latex gloves for determining the efficacy of PMMA-coated sensors [161,217]. PDMAEMA is a synthetic cationic polymer that acts as a copolymer and is linked with poly (dimethyl aminoethyl methacrylate) - poly(e-caprolactone) - poly (dimethyl aminoethyl methacrylate) *in-vitro* studies causing antimicrobial activity owing to its bactericidal activities [163,218]. The PMs loaded with no drug and curcumin caused upregulation of oxidative stress markers malondialdehyde (MDA) and glutathione (GSH) and depicted that

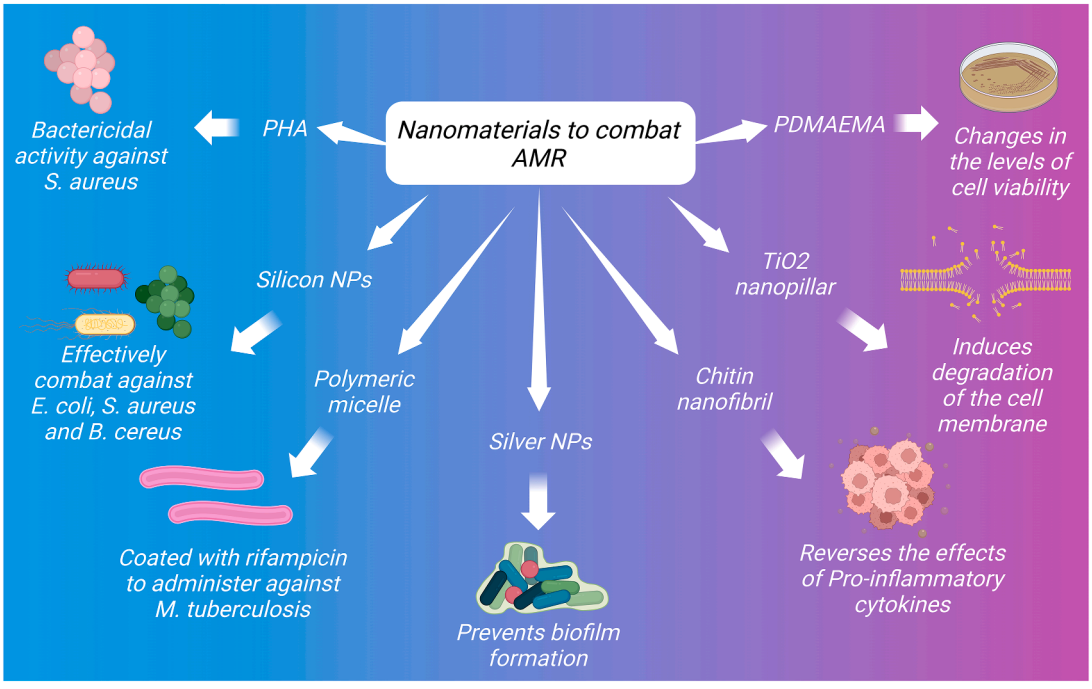

Fig. 8. Schematic model provides an understanding of nanomaterials' application against AMR.

Table 1
Application of NMs for anti-microbial activity.

NMs	Characteristics	Functionalization	Type of preclinical study	Result	References
Silicon NM	Negative charges, anti-cohesive properties and biocompatible	Nanospikes of black silicon has bactericidal activity and black silicon is also used in the development of microfluidic device.	Both *in-vivo* and *in-vitro*	Effectively combat against *E.Coli, S.aureus* and *Bacillus cereus.*	[150,188]
Chitin nanofibril (CN)	Anti-inflammation, anti-bacterial, cationic and hydrophobic	Administered into human keratinocytes.	*In vitro*	Counter-reverses the effects of pro-inflammatory cytokines such as TNF-α, IL-6, IL-1α, and IL-1β.	[210–212]
Polyhydroxyalkonates (PHA)	Biocompatible biocidal activity, Bioresorption substitute for petroleum-producing plastics	PHA integrated with sulfur groups and thioester moieties (PHACOS) interact directly with microbes.	*In vivo*	Biocidal activity against *S. aureus.*	[213]
TiO2 Nanopillars	Produces ROS, anti-microbial activity	They induce degradation and penetration of the cell envelope of gram-negative and gram-positive bacteria.	*In vivo*	TiO2 nanopillars generated oxidative stress against *S.aureus* and *E.coli* cause anti-microbial activity.	[157,242]
PMMA functionalized material	Biocompatible, anti-inflammatory and N ontoxic	orthopedic implants and latex gloves are PMMA functionalized.	*In vivo*	Downregulation of cytokines such as IL-1β, IL-6, and TNF-α and reduced migratory inhibitory factor (MIF) for cytotoxic effect.	[243]
Poly (2-N, N-dimethylaminoethylmethacrylate) (PDMAEMA)	Cationic polymer, biocompatible and bactericidal activity	Acts as a copolymer and is linked with poly (dimethylaminoethyl methacrylate) - poly(e-caprolactone) - poly (dimethylaminoethyl methacrylate).	*In vitro*	Polymeric micelles loaded with curcumin showed the characteristic change in levels of oxidative stress markers malondialdehyde (MDA) and glutathione (GSH) and also depicted those cationic micelles do not elicit changes in cell viability.	[163,218]
Cationic Liposome	Biocompatible, cationic and anti-bacterial activity	Coating cefepime when administered against *E. coli* post-encapsulation by vesicle.	*In vitro*	Inhibits infections caused by *E. Coli.*	[168]
Proliposome	Antimicrobial activity and biocompatible	Coating proliposome with cefquinome sulfate and conjugation of antibiotic with the vesicle achieved by solid dispersion method for effervescent hydration.	*In vitro*	Administered against *S. aureus.*	[170]
Polymersomes	Hydrophilic, enhanced circulation time and high loading capacity	PEG functionalized polymersomes act as block copolymer amphiphile.	*In vivo*	Act against plasma proteins.	[227–229]
Polymeric micelles	Hydrophobic, low density, bioinert, greater efficiency and negligible toxicity	Polymeric micelles were coated with rifampicin.	*In vitro*	Administration against *M. tuberculosis.*	[177]
Nanodiamonds (NDs)	Bactericidal activity	NA	Both *in-vitro* and *in-vivo*	It shows bactericidal activity against *E. coli* and *S. aureus.* NDs tailored with amoxicillin led to the internalization of uropathogenic *E. Coli* habituating T24 bladder cells, which manifested bactericidal activity.	[181,182, 231]
Polyethyleneimine (PEI)	Highly branched structure, cationic and biocompatible	NA	*In vivo*	Nucleus-targeting gene delivery systems *via* binding to cytoplasmic receptors and further translocating to the nucleus causing anti-microbial activity.	[218]

cationic micelles do not elicit changes in cell viability [218].

A liposomal encapsulated vancomycin and vancomycin hydrochloride was administered in *S. aureus* and methicillin-resistant *S. aureus* (MRSA) for antimicrobial activity. The conjugation of antibiotics with vesicles was prepared by freezing, thawing, and reverse-phase evaporation, highlighting the importance of MLVs as hydrophobic antibiotics and unilamellar vesicles (LUVs) as hydrophilic antibiotics [219]. In another study, vancomycin was administered using polymersomes conjugated by sonication MRSA for developing hyaluronic acid-oleylamine (HA-OLA) conjugates as a nanocarrier for antibacterial activity *in-vitro* studies. With a 25–50% degree of conjugation, the nano-drug conjugate material exhibited antibacterial activity with potency at MIC of 500 μg/mL by an estimated drug release post 72 hrs [220]. Moreover, a cationic liposome coating cefepime, when administered against *E.coli* post-encapsulation by vesicle, exhibited anti-microbial activity. The cationic structures were characteristic of cationic surfactant, *N, N, N*-triethyl-*N*-(12-naphthyl dodecyl) ammonium. The efficacy of liposomes tethered with phosphatidylcholine and cholesterol is more proficient than 1,2-dioleoyl-*sn*-glycero-3-phosphoethanolamine (DOPE) thereby validating the biocompatibility of cationic liposomes against inhibition of bacterial infections caused by *E.coli* [168]. A pro-liposome coating functionalizing with cefquinome sulfate was administered in *S. aureus* with conjugation of antibiotics by solid dispersion method for effervescent hydration to cause anti-microbial activity [170].

Polymersomes predominantly accumulated in the liver of *in-vivo* rat models where PEG-based copolymer amphiphiles retained double circulation time compared to non-PEGylated vesicles [221]. PEG acted as a hydrophilic surface layer for polymersomes that induced the suppression of interfacial free energy and minimized steric repulsions causing augmented blood circulation times [222–224]. The preference for PEG-based copolymer over PEG-modified lipid vesicles roots from the limited potential of these lipid vesicles in their stable integration owing to the curvy structure and bulk hydrophilicity conferred by the large chains of PEG which incorporate as a small proportion of the lipid membrane in the form of micelle-forming amphiphiles [225,226]. However, polymersomes augment the hydrophobic fraction and develop an enhanced loading capacity along with conferring higher resistance against plasma proteins [227–229]. PEE is tagged as a hydrophobic block with low density and is commonly used in medical implants owing to its bioinert nature [230]. PM-coated rifampicin was used for administration in *Mycobacterium tuberculosis* via encapsulation by solvent diffusion. This nanocarrier used a graft-copolymer of poly (vinyl caprolactam)-poly (vinyl acetate)-poly (ethylene glycol) (Soluplus) that is available commercially for more efficient drug delivery to the lungs with low toxicity [177].

The nanopillars enabled structural re-organization and infiltration into the envelope of gram-positive and gram-negative bacetria induced oxidative stress to inhibit bacterial cell division and reduce cell viability. Oxidative stress against *E. coli and S. aureus* was generated by TiO_2 nanopillars to cause anti-microbial activity [157]. TiO_2 nanopillars were designed to induce degradation and penetration of the cell envelope of gram-negative and gram-positive bacteria inspired by nano protrusions on dragonfly wings. They possess the potential to inhibit bacterial replication and produce oxygen species without causing cell lysis [157]. Nanodiamonds are another fascinating NMs exhibiting anti-microbial activity. The action potential of nanodiamonds (NDs) exhibited bactericidal activity by inducing deformation of the bacterial cell (*E. coli*) by establishing a direct correlation between the oxygen levels and bacterial death for partially oxidized surfaces equipped by nano-diamonds [181]. Moreover, the bactericidal characteristics of NDs exhibited against *S. aureus* by limiting biofilm formation for antimicrobial activity based on bacterial size, structure, concentration, and exposure duration [182]. Iyer *et al.* exhibited that the impact of NDs tailored with amoxicillin led to the internalization of uropathogenic *E.Coli* habituating for bactericidal activity post 2 hours of administration of the ND conjugated system [231]. For therapeutic applications, it is essential to comprehend the cytotoxicity, which has been primarily addressed *in-vitro* studies [232]. However, *in-vivo* studies needed to be performed to understand better the biological effects of these suggested NMs, including biodistribution, metabolism, toxicity, clearance, and mechanism of action, before any clinical practice.

5.2. Surface topology-based nanomaterials

Surface topology-based Nanomaterials are explored in a considerably large population of marine animals gifted with placoid scales and wavy topological dimensions owing to their hydrodynamic properties. Certain factors enhance the efficacy of anti-fouling polymers, such as contact angle with water droplets at the polymer's surface that affects the adhesion dynamics [185]. Self-mediated cleansing is attributed to the superhydrophobic nature of these materials induced by their leaf-like structural configurations [185]. Artificial or synthetic designs of materials ranging from devices constituting thermoplastic polyurethane polymers to polydimethylsiloxane, expressing antifouling properties, have led to the commercialization of several products with diagnostic applications [191]. The antifouling activities exhibited by zwitterion are attributed to their low surface energy, structural properties, and chemical stability, thereby paving the way for widespread applications in tissue engineering and graft modeling [185]. A conical nanostructure patterned wing showing evolutionary adaptation exhibited antimicrobial activity against *Pseudomonas aeruginosa* utilizing antimicrobial activity [233].

The high aspect ratio of nano-pillars and high motility of the bacteria elevated the antimicrobial activity by assuring a perpetuated exposure of the bacteria with the nanostructures, eventually exceeding the shear stress to cause lethal repercussions. The nanostructures characterized by structural deviations differ from each other and impart distinct bulk properties to each of the materials, as mentioned above, irrespective of the physicochemical properties [234–238]. Hence, they are mutually exclusive in terms of their characteristics, and designing these structures is loaded with an additional cost. Studies have shown that insect wings and physical nano protrusions synergistically exhibit bactericidal activity against *Branhamella catarrhalis, E. coli,* and *Pseudomonas fluorescens* [234–238].

Antimicrobial peptide polymers exhibit significant efficacy against the microbial population and are subdivided into classes, out of which each polymer corresponds to specific peptides. AMP acts as defense agents against microbial pathogens, and the characteristics

that represent an ideal AMP are their size which should range between 6–59 amino acids, sequencing with the ratio of hydrophobic to a charged concentration 1:1 or 2:1, configuration and amphipathicity or their hydrophobic moment [239]. Bacteria are known to exhibit resistance against these peptides by a mechanism that involves the secretion of proteolytic enzymes by the bacterial cell walls leading to hydrolysis of these peptides. This can be supported by *S. aureus,* which can either alter the net surface charge, thereby restricting entry of AMP or it can manifest active efflux transporters supported by the synergistic effect of proteolytic enzymes like metalloproteinase (aureolysin) to develop resistance against AMPs [240]. Novel NMs, also known as star peptide polymers, are multivalent antimicrobial peptide polymers (SNAPPs) with structurally nano-engineered antimicrobial peptide polymers (SNAPPs). *In-vivo* studies have shown that these nontoxic nanocarriers improve antimicrobial drugs' biocompatibility, stability, and therapeutic efficacy [241]. Maximum H5 and Dermcidin peptides conjugated with anionic polymers originated from amphibians and humans for anti-microbial activity. Some other examples include cecropins, andropin, moricin, ceratotoxin, and melittin are peptides conjugated with linear cationic and α-helical polymers originating from insects for anti-microbial activity. 2-disulfide bridges (protegrin) and 3-disulfide bridges (α-defensins) are conjugated with anionic and cationic polymers containing cysteine with disulfide bonds originated from pigs and humans (HNP-2) whereas proline containing abaecin and tryptophan containing indolicidin were conjugated with cationic polymers enriched with specific amino acids that originated from honeybee cattle for anti-microbial activity [241].

6. Membrane camouflaged NPs

Cell membrane coatings are a promising approach towards camouflaging which ensures the localization of the protein of interest in a native environment compared to the membrane-associated proteins. These formulations are represented by complex chemistry and can dodge the immune system. For such purposes, RBCs are commonly preferred due to their prolonged circulation time and biconcave shape, having the potential to undergo deformation and feasibly pass the capillaries [244]. The limitations equipped with using artificial cell membranes directionalized the application of cell membrane coating of NPs, which was first observed in case of natural deformation of RBC to continue prolonged circulation in the blood, membranes of WBC, platelets, and cells without nuclei in the same applications [245–249]. In a similar study by Jarvi *et al.*, an anionic NP ranging in diameters between 50–200 nm was coated with negatively charged cell membranes where the cell membrane source can either be obtained from cultured cells for anti-microbial activity [250–253].

RBCs permit easy cell membrane extraction due to decreased magnitude of cell debris and reduced purification steps [254]. The preparation of RBC-coated membrane camouflaging by NPs is mainly focused on isolating RBCs from the WBCs and projecting them to a hypotonic environment which empties the cell and permits the RBC membrane to be developed. This membrane will most likely be fused with PLGA-NPs *via* mechanical extrusion for targeted delivery for antimicrobial activity [255]. Fullerene-based NPs coated the RBC cell membranes for effective theranostics against thrombosis with greater efficacy in rat models [244]. In addition, RBC membranes are equipped with CD47 protein, which shields the cells from lysis and degradation, resulting in higher retention ability [256]. Bacteria-coated RBC rendered 14 times magnified retention potency *in-vivo* murine models with a target of dodging immunogenic response in targeted cells where the bacteria coated with RBC membrane manifested 14 times higher retention compared to uncoated bacteria within a span of 48 hrs in murine models. These coatings are incorporated with inflammatory markers, which tend to dissolve upon bacterial cell division [257].

The hepatic and renal clearance of NPs curbs the formation of membrane-mediated cytotoxicity in the targeted site. These NPs are identified by the immune systems while characterizing unique physicochemical properties such as size, surface hydrophilicity, surface charge, and geometry, causing enhanced accumulation and biocompatibility for advancements in biomimetic nanoengineering [258]. These NPs play a significant role in therapeutic applications such as blood circulation, immune evasion, ligand recognition for vaccination, detoxification, and drug release. The coating of lipid-tethered entities by RBC membranes allowed NPs to potentially target ligands, of varying mass as the dynamics of the bilayer elicited the expression of small as well as macromolecular proteins onto the RBC surface without interfering with the previously existing membrane proteins. Hence, the lipid introduction proved an effective and robust way to deliver biomimetic nanocarriers [247,258].

Hence, we can infer that cell membrane-coated NPs and NPs having a synthetic core act as adjuvants with minimal adverse side effects. While one provides an intrinsically homing environment, the other potentially redeem the multifaceted targeting efficacy and

Table 2
Application of Membrane coated NPs for antimicrobial activity.

Membranes	Characteristics	Functionalization	Clinical Study	Results	Ref.
NP coated with negatively charged RBC cell membrane	Size (50–200 nm) Anionic NP	The membrane is most likely to be fused with PLGA NPs via mechanical extrusion for targeted delivery of antimicrobial activity.	*In-vivo* and *In-vitro*	NP coated with cell membrane shows antimicrobial activity. It also provides theranostics against thrombosis with greater efficacy in rat models.	[250–256]
Lipid NP coated with RBC cell membrane	Lipid NP Biocompatible	Coating of lipid-tethered entities by RBC membranes allowed NPs.	*In vitro*	It allows NP to potentially target ligands of varying mass as the dynamics of the bilayer elicited the expression of small as well as macromolecular proteins onto the RBC surface without interfering with the previously existing membrane proteins.	[247,258] [259]

confers a hold over the drug pharmacokinetics [259]. The clinical significance of membrane-camouflaged NPs is summarized in Table 2.

7. Nano device and nanomachines

Despite improved therapeutic approaches in the biomedical industry, the drawbacks of post-surgical contamination in clinical devices yet continue. These devices challenge the influential functional role of antimicrobial polymers by triggering a strong immune reaction. Some commonly known devices leading to the same would include urinary catheters, vascular catheters, prosthetic cardiac valves, endotracheal tubes, orthopedic implants, endotracheal tubes, and contact lenses [260]. A rational alternative would be utilizing surface-coated intrinsic antimicrobial or antifouling polymers acting against bacterial infiltration. These implants can also be developed by artificial intelligence and evolved into robotic devices, which will cause deteriorated biocompatibility. Several techniques to subside the side effects of implants would include increased cost or risk factors [261]. Tissue fibrosis and capsular contracture act as hurdles in the procedure of surgical intervention post-reimplantation. Hence, antimicrobial coating in these materials is associated with skin damage, nasal septum, and bone-anchored hearing aids in ear implants and serves as a practical alternative therapeutic approach by acting as a protective layer against infection. They aid in self-induced tissue regeneration while minimizing the urgent need for the surgical procedure.

When technological tools such as 3D printing, stereolithography, and hydroxyapatite-based composites are forwarded toward us, a giant leap towards faster utilization of these biomedical devices in the prognostic sector is taken against MDR pathogens [261]. An initiative to combat the MDR bacteria was taken by the molecular nanomachines (MNMs) that potentially perforate the bacterial cell wall to deliver the drug and counter the inefficacy of antibiotics. With the mounting tension of infections, it is important to replace conventional antibiotics with high throughput devices to augment the susceptibility of drugs against MDR bacteria [262,263]. The molecular nanomachines possess rotor components that foster light-activated functioning to induce rotation unidirectionally while their rotational mechanics degrade the cell membrane and the lipid bilayer to allow drug penetration [264–266]. The clinical significance of nanorobots and nanomachines are highlighted in Fig. 9 and Table 3, respectively.

A study by Galdbage et al. demonstrated nanomachines' role in administering meropenem, a specialized drug for treating skin and

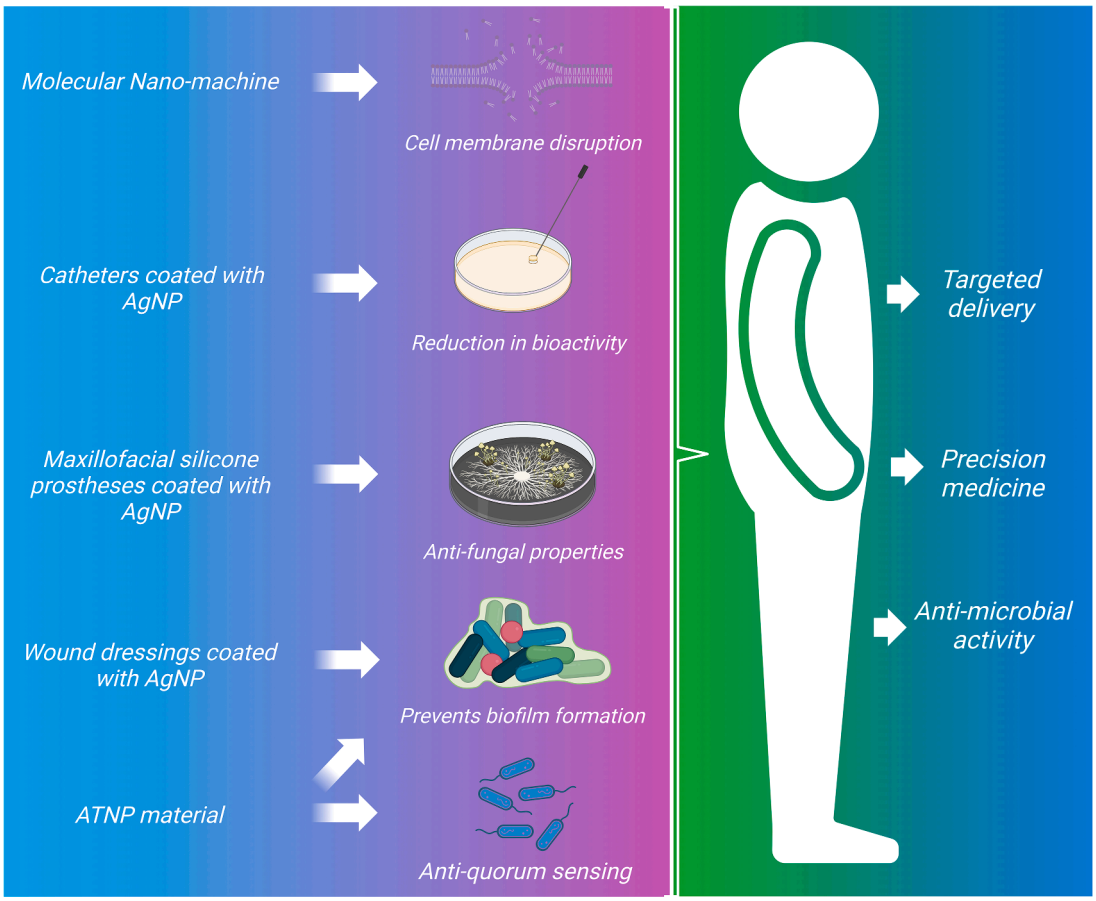

Fig. 9. Graphical model providing an understanding of the theranostics properties manifested through the action of nanorobots and nanomachines causing anti-microbial activity.

Table 3
Application of nanodevices for antimicrobial application.

Nanodevice	Characteristics	Functionalization	Clinical Study	Result	Ref.
Molecular Nano-Machine (MNM)	Synthetic organic nano-molecules conjugated with Meropenem 365 nm light source to activate MNMs.	Cell walls of ψkp6 (AR-0666) and ψkp7 (NIH-1) strains of *K. pneumoniae* were subjected to drilling by the MNMs.	*In vitro*	The aim of inducing bactericidal activity in MDR pathogens by increasing the intracellular concentration of antibiotic (Meropenem) using light-activated MNMs was effectively conducted.	[271]
Wound dressings coated with silver NP	a) Mepilex^{R} Ag having dense silver sulfate (Ag2SO4) dressing with a tender foam of silicone [Silver]. b) Inadine^{R} having a PEG base with knitted viscous fabric and 10% povidone-iodine [Non-Silver].	Manifests 100 percent reduction in biofilm biomass with a p-value – 0.001 against the two isolates- *Pseudomonas aeruginosa* and *Acinetobacter baumannii.* Manifests 3 percent addition in biofilm biomass with a p-value – 1.000 against the aforementioned isolates.	*In vitro*	Significant variation observed in the ability to prevent biofilm formation where silver-coated dressings (Mepilex^{R}) have manifested complete prevention in contrast to non-silver-coated (Inadine^{R}).	[273]
Catheters coated with silver NP	Medical grade vacant silicone sheet 0.45 mm thick segmented into discs of 15 mm diameter organic complexes of silver impregnated into silicon discs.	Clinical isolate of *Staphylococcus epidermidis* was subjected to inoculation with 50 % human plasma-coated impregnated discs which had two sets – one set washed after impregnation, and the other was directly coated with plasma.	*In vitro* and *In vivo*	Silver-coated silicone elastomer showed a reduction in the inhibition zone of bacterial culture from 8.5 mm on day 1 to 3 mm on day 5 in the case of unwashed discs thereby confirming the absence of residual bacteria. No inhibition zone was observed in the case of washed discs thereby validating the antimicrobial activity of the catheters.	[274]
Maxillofacial silicone prostheses coated with silver NP	Medical grade silicone discs (37 mm in diameter, n 5 6/treatment) coated with 5 and 50 mg L−1 dispersions of Ag NPs and $AgNO_3$ and prepared using a platinum-catalyzed, vinyl-terminated poly(- dimethyl siloxane) elastomer (A-2186, Factor II, Lakeside, AZ, USA).	Biocompatible concentration of Ag NPs was compared to $AgNO_3$. The effect of AgNPs-coated silicone elastomer surface was studied in fibroblast cells and antifungal properties of silver-coated silicone elastomer against *C. albicans* were tested in the presence of fibroblast cells.	*In vitro* and *In vivo*	Ag (13 mg L^{-1}) was detected from the AgNO3 coatings in the media, but total Ag remained below the detection limit (<1.2 μg L^{-1}) for the Ag NP coatings which depicts the higher stability of AgNP. Silicone prosthetic materials coated with Ag NPs are biocompatible with fibroblast cells *in vitro* and show antifungal properties.	[277]
Polymer–graphene oxide composite	Polyvinyl-N-carbazole (PVK)–graphene oxide (GO) nanocomposite (PVK–GO) containing 3 wt% of GO well-dispersed in 97 wt% PVK matrix.	Toxicity of PVK–GO was evaluated with planktonic microbial cells, biofilms, and NIH 3T3 fibroblast cells against two Gram-negative bacteria: *E. coli* and *Cupriavidus metallidurans*; and two Gram-positive bacteria: *Bacillus subtilis* and *Rhodococcus opacus.*	*In vitro*	PVK– GO is toxic to mammalian cells, bacterial planktonic cells, and biofilms which validates its suitability as an anti-microbial agent in the biomedical and industrial domain without inflicting any harm to human cells.	[276]
ATNP material	AgCl-TiO2 nanoparticles (ATNPs) with 1 (wt) % silver Sterile discs (6 mm diameter) were impregnated with different concentrations (100, 200, 300, 400, and 500 μg) of ATNPs TiO2 without silver (500 μg) was used as the control.	ATNPs were inoculated with *Chrobacterium violaceum* ATCC 12,472 wild-type strain which produces autoinducer molecules like AHLs that are responsible for producing a violet-colored pigment known as violace.	*In vitro*	ATNPs inhibit pigment production by *C. Violaceum* and hence confer excellent antimicrobial as well as anti-quorum sensing activity (increase with increasing concentration of ATNP- from 100 μg to 500 μg ml^{-1}) against Gram-positive and Gram-negative micro-organisms. Biofilm inhibition was observed at anti-QS concentration without affecting the viability of the cell.	[278]
Graphene-coated composite with titanium	Graphene-based silver/hydroxyapatite/graphene (Ag/HAP/Gr) composite coatings produced by electrophoretic deposition (EPD) on titanium Graphene was incorporated in HAP	Ag/HAP/Gr coating on Ti was used to study the cell viability of peripheral blood mononuclear cells (PBMC). The antibacterial activity of Ag/HAP/Gr coating was tested against	*In vitro* and*In vivo*	Antibacterial activity against *Staphylococcus aureus* and *E. coli* was manifested along with non-cytoxicity against healthy PBMC, allowing the scope in futuristic biomedical applications.	[279]

(*continued on next page*)

Table 3 (*continued*)

Nanodevice	Characteristics	Functionalization	Clinical Study	Result	Ref.
	[Hydroxyapatite, $Ca_{10}(PO_4)_2(OH)_2$], and the thickness of graphene nanoflakes was 12 nm. A nano-sized Ag/HAP powder was prepared with a silver concentration of 0.4 ± 0.1 wt.%.	Gram-positive pathogenic bacteria strain *Staphylococcus aureus* and Gram-negative bacteria strain *E. coli.*			
Dentifrice coated with silver fluoride	Nanosilver fluoride (NSF) is characteristic of AgNPs and fluoride AgNPs appeared as mono-disperse particles that were 8.7 ± 3.1 nm in diameter.	Dentifrice containing nano-silver fluoride (NSF) and sodium fluoride (NaF) toothpaste were subjected to *in vitro* analysis against cariogenic bacteria *Streptococcus* mutants to determine the minimal inhibitory concentration (MIC), minimal bactericidal concentration (MBC).	*In vitro*	MIC of the dentifrice test using NSF was 30 ppm, whereas MIC of the same test using NaF was 180 ppm. Dentifrices containing NSF manifested a lower MIC and better results compared to NaF dentifrices. Hence, it can be concluded that NSF is significantly better at preventing bacterial adhesion and performing antibacterial activity.	[280]

abdominal infections caused by bacteria in *Klebsiella pneumoniae*. The major challenge presented by this species was the loss of porins and the subsequent production of *K. pneumoniae carbapenemase* (KPC) [267–270]. Furthermore, the viability of bacterial cells was reduced by 14–17% by the incorporation of light-activated MNM using meropenem at subtherapeutic concentrations [271]. Hence, these medical devices must be subjected to sufficient *in-vitro* studies to deduce plausible ways of their effective commercialization and theranostic application.

In a similar investigation, Halstead et al. depicted the influential role of a wide spectrum of dressings to hinder biofilm formation induced by burn wound pathogens such as *Enterobacter spp, K. pneumoniae, E. coli, E. faecalis, S. aureus, A. baumannii,* and *P. aeruginosa*. Furthermore, the action potential of silver-containing dressings was evaluated in a recent study using randomized controlled trials of silver dressings. Comparative analysis was conducted against non-silver dressings, which exhibited that silver dressings were relatively significant in healing burn wounds [272]. Similarly, in a study by Fan et al., wound dressing using hydrogel, which could perform an antibacterial activity, was aimed at sustaining the water and maintaining capacitance to retain moisture around the wounds. The formation of hydrogel panels by crosslinking Ag/graphene composites possessing acrylic acid and N, N′-methylene bisacrylamide at varying mass ratios were evaluated *in-vivo* with appreciable biocompatibility and flexibility to enhance the healing rate of wounds in murine models effectively. Thus, rendering the use of these dressings is a reliable option against wounds induced by MDR pathogens [273].

A novel approach has been applied using supercritical carbon dioxide to impregnate silicone with AgNPs to overcome the complexities associated with biomaterials coated with silver oxide or silver alloy and ultimately foster antimicrobial activity. The futuristic use of this method as an antimicrobial biomaterial is an arena with a possible scope of advancements against AMR [274]. Duran *et al.* demonstrated that using microorganisms such as *Fusarium oxysporum* enabled the remediation of toxic metals such as silver which can be reduced extracellularly to generate stabilized and effective silver (or gold) NPs in water. These NPs possess the potential to inhibit healthcare-associated infections (HAI) by impregnating cotton fabrics that exhibit antimicrobial activity against *S.aureus,* and the effluent was bio-remediated using *C.violaceum*. Thus, these NPs were developed into AgNCs fibers, rendering sterility to these clothes by acting as a water filter by deducing the bacterial output load to a null amount [275].

Carpio *et al.* highlighted the application of graphene-based nanodevice consisting of polyvinyl-*N*-carbazole (PVK)–graphene oxide (GO) (PVK-GO) with high polymer content to allow high-yield manufacturing of adiabatic bulk polymerization. A significantly higher antibacterial activity by suppressing the metabolic activity of *E. coli, Cupriavidus metallidurans, Bacillus subtilis,* and *Rhodococcus opacus* cells leads to cell lysis without causing any toxicity and thereby acts as a promising candidate in the field of biomedical devices [276]. The assembly of bioactive homogenous coatings was formed by electrophoretic deposition (EPD) of graphene-based silver--hydroxyapatite on titanium that led to enhanced antimicrobial efficacy of graphene for toughening action, higher mechanical resistance and augmented thermal stability against *S. aureus* and *E.coli.* Ag/HAP/Gr exhibited high bioactivity with the formation of an appetite layer in simulated body fluid with corrosion stability and minimal cytotoxicity in healthy peripheral blood mononuclear cells (PBMC) [260].

8. Nano-antibiotics

Metal oxide, metal-based NPs incorporated with antibiotics pave the way for the implementation of augmented antibacterial as a promising alternative having theranostics potential [281,282]. The dissolution of efficacy and biocompatibility are owed due to their size-to-volume ratio that allows the NPs to foster targeted drug delivery via degradation of the bacterial cell membrane, suppression of biofilm, elicitation of reactive oxygen species (ROS), regulation of immunogenic response and disintegration of host DNA and proteins [283]. Nano-antibiotics have the potential to emerge as pillars of biomolecular entities generating a positive response against the therapeutics of MDR bacteria [284]. A recent study demonstrated that bismuth NPs decelerate the pace of rapidly spreading MDR

Candida auris strains while providing scope for more insights into the pharmacology, action accuracy, and controlled usage of antibiotics for guaranteed safety and effective drug delivery in the biomedical field [285]. The waning effects of traditional antibiotics are counterbalanced by perpetual attempts at discerning cutting-edge technologies that enable less dependence on synthetic therapeutics [284]. The advent of MDR ubiquitous bacteria and other microbes has posed a life-threatening challenge for researchers to combat the

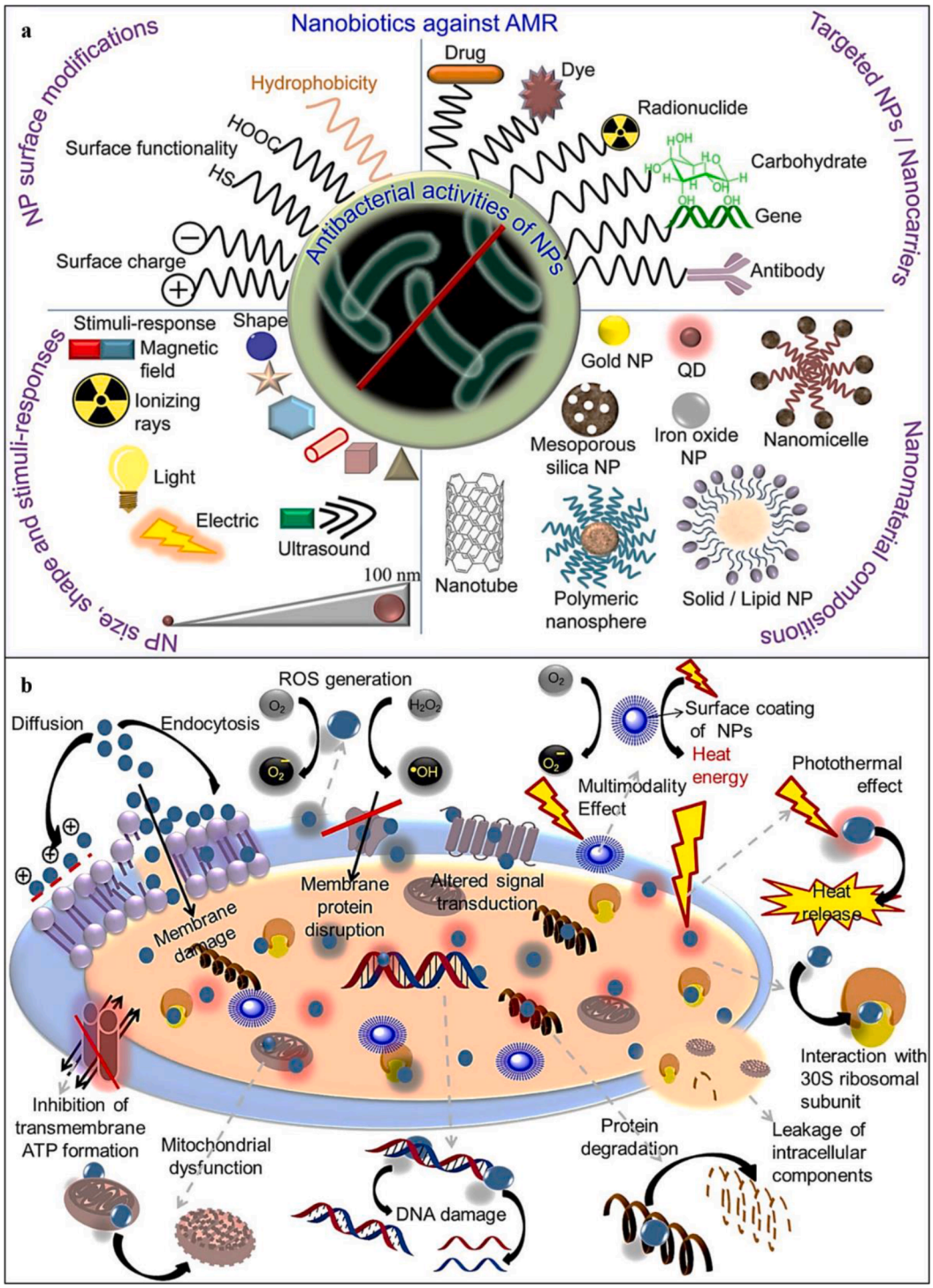

Fig. 10. (i) Graphical model providing nano theranostic-based anti-microbial activity through surface modification, size, composition, and induces stimuli of nanoparticles. (ii) Mechanistic profiling of strategies to combat MDR pathogen *via* nano-antibiotics-based synergistic action. Adapted with open access permission from [233].

Table 4
Application of nano-antibiotics for anti-microbial activity.

Nano-antibiotics	Nanosystems	Characteristics	Functionalization	Type of Preclinical Study	Result	Ref.
Penicillin-G (PenG)	Silica NPs	PenG conjugated with dye-labeled sNPs -15 nm diameter characterizing carboxyl groups located as either surface-functional groups or on polymer-chains (PMAA) extending from surfaces using RAFT polymerization. The mean diameter of bare NPs was 18.9 × 0.4 nm, and that of carboxylic acid coated-NPs was 22.7 nm.	The NPs conjugated antibiotic was tested against *E. coli, S. Aureus* and methicillin-resistant *S. aureus* (MRSA) strains. PenG was randomly tailored to monolayer carboxylic acid or PMAA grafted sNPs via physical interactions.	*In vitro*	Unbound penicillin had null antimicrobial activity; however, the nanocomplexed form of penicillin with the same dose of PenG (0.25 μl) showed augmented microbial activity verified by its presence in the inhibition zones of agar plates.	[292]
Ampicillin	AuNPs	Three isotopes of Au are taken – Au (100), Au (110), and Au (111). Adsorption of the antibiotic occurred at the S atom/N atom with the Au NP.	AuNP/AMP relies on several facets, including adsorption energies, bond distances, and electron densities, to combat strategies against ampicillin-resistant bacteria.	*In vitro*	Highest stability of conjugation was observed in Au (110) owing to their adsorption energies. AuNP/AMP allows the antibiotic to inhibit the efflux pump which avoids the deactivation of antibiotic by β-lactamase resulting in a higher concentration of antibiotic in the bacterial cell.	[293]
Tetracycline	Silica NPs	Encapsulation of tetracycline (TC) antibiotic in nanostructures similar to Mesoporous silica nanoparticles (MSN). SiO_2-TC composites are quasispherical NPs with an average size of nearly 60 nm.	The antimicrobial efficacy of bare silica nanoparticles (control – SiO2) and silica-tetracycline nanoparticles (SiO_2-TC) was evaluated against tetracycline-susceptible and multiple resistant *E. coli*. The NPs cytotoxicity was evaluated against HEK 293t mammalian cells.	*In vitro and in vivo*	No colonies were observed for SiO_2-TC and free-TC in the case of susceptible *E.coli.* The percentage of surviving colonies for TC-resistant *E. coli* for SiO_2 and SiO_2-TC was 32.3 ± 3.6% and 34.7 ± 18.3%, thereby showing the decrease in percentage survival of bacterial colonies, which validates their efficacy as promising nano-antibiotics.	[294]
Caesalpinia sappan	Ag NPs	NPs were spherical and amorphous with diameters ranging from 30.2 to 47.5 nm.	The conjugated system was synthesized from *C. Sappan* was coated with stabilizers to test antimicrobial activity against MRSA.	*In vitro*	*C. sappan* methanol extracts were known to exhibit antioxidant, anti-inflammatory, and antibacterial activity and had MIC values ranging from 75 to 150 g/mL. Addition of stabilizers (CTAB) enhanced antibacterial activity by acquiring MIC ranging from 18.75 to 75 μg/mL.	[295]
Ampicillin, Oxacillin, Linezolid, and Vancomycin	AuNCs	AuNCs functionalized with quaternary ammonium with an average size of 2 nm.	The antibacterial activity of the QA-AuNCs towards *S. aureus* was evaluated against ampicillin, oxacillin, linezolid, and vancomycin in murine models.	*In vivo and in vitro*	Excellent biocompatibility was established by AuNCs both *in-vivo* and *in-vitro*. The QA-AuNCs with vancomycin are most effective in eradicating MDR bacteria.	[296]

pathogenic remnants, as shown in Fig.10.

The extraction process of AuNPs using physical and chemical methods has faced several setbacks leading to faltered efficacy towards truncating antimicrobial resistance; some include the rising expenditure of synthesis of NPs, adverse side effects linked with cytotoxic effects, high polydispersity and ultimately deteriorating yield [286–288]. Hence, the central focus of research revolves around developing nontoxic, minimally costly, and highly stable systems [289].

The NPs have been reported as competent carriers for the targeted delivery of antimicrobial agents. The physicochemical properties, including smaller size, larger surface area-to-mass ratio, tuable shape, size, and surface charge NPs, make them potential strategies to eradicate microbes. The nanoparticle-conjugated antimicrobial therapeutic strategies exhibit various molecular mechanisms for the effective eradication of the microbial flora. These include disruption of the cell membrane, upregulation of ROS production leading damage of DNA, causes oxidative stress within microbial environment, inhibition of several enzymes, protein deactivation, alteration of gene expression, and others [233].

A study by Emmanuel et al. depicted the role of AuNPs synthesized from *Justicia glauca* conjugated with Azithromycin (AZM) and Clarithromycin (CLR) antibiotics against varied strains of bacteria and fungi including *C. albicans, P. aeruginosa, L. acidophilus, Pseudomonas sp, E. coli,* and *S. aureus*. The examination and characterization of these green synthesized AuNPs were conducted by conjugating NPs that manifested significant antimicrobial activity by exhibiting a MIC of 6.25 - 25 μg/mL against the bacterial and fungal pathogens [290,291]. They pave the way for the futuristic implementation of antimicrobial therapy post-validation of effective prognostic potency from *in-vitro* and *in-vivo* studies. Thus, it is essential to incorporate the conjugated NPs to ensure the targeted delivery of drugs since conventional antibiotics are burdened with the backlogs of resistance and elicitation of unfavorable side effects such as allergic reactions, hypersensitivity, and immune suppression. Further, the studies reported with potential theranostic applications of NPs-conjugated antibiotics with improved anti-microbial activity is discussed in Table 4.

9. Potential nano-toxicity of nano-systems used for anti-microbial activity

Nanotoxicity is strongly correlated with the narrow size distribution, high surface area to mass ratio, and surface characteristics of NPs. Furthermore, NPs can invade cell and tissue membranes, causing cellular damage and toxicity. Therefore, it is of utmost concern nowadays to investigate the processes of nanotoxicity, despite having unique characteristics at the nanoscale that set the NPs apart from their bulk and dissolved counterparts. Metals exhibit this unique activity in a way that not only offers significant benefits but also harms because of their unintended interactions with various cellular functions.

The toxicological effects of SiNPs were investigated, where test species, including mollusks and fish embryos, were used. And by observing the heart rhythms in the embryos of *Danio rerio* mussels, it was demonstrated that SiNPs with a mean size of 2–4 nm were hazardous [297]. Based on the LC50 value, it was discovered that fluorinated radicals, rather than the SiNP inherent toxicity, were the primary cause of the nanotoxicity [298]. Furthermore, it was established that these particles directly caused a delay in embryo development and larval deformity [298]. Since dilution, dissipation, and uptake by hydrobionts occur throughout an organism's life cycle, ecological studies must ascertain the long-term effects of NPs' impact on hydrobionts at relatively low toxicant concentrations [298]. On the surface of the SiNPs, which ranged in size from 1.8 to 5 nm and had various functional groups, detrimental toxic effects on the embryos were examined [298]. During the first 96 hours after conception, the embryos were tested for survival rates, morphological flaws, and developmental delays. Some researchers discovered that human mesenchymal stem cells were toxic to SiNPs in terms of their metabolism, survival, adhesion, proliferation, migration, oxidative stress, and ability to differentiate [298].

When discussing CN, due to the intriguing, unique properties of CN and lignin, CN-LG NPs have been developed to be used as functional carriers of active substances for the regeneration of human tissues [299–301]. Significant efforts have been made to create non-woven tissues that replicate the behavior of the skin for this purpose. Numerous investigations have demonstrated that CNs do not form when the crystals have high crystallinity and submicrometric size [299–301]. CNs can cause chitin's allergic characteristics and inflammatory activity. Additionally, since physiological enzymes like lysozyme and chitinases may spontaneously break them down, CNs do not pose a significant risk for nanotoxicity [299–301].

PHAs are up-and-coming materials to replace the non-degradable polymers manufactured from fossil fuels because they are biodegradable and biobased polyesters [302,303]. Systems metabolic engineering will make it possible to optimize metabolic fluxes at the genome-wide level, which will improve the manufacture of PHAs and synthetic polyesters from low-cost substrates with improved PHA titers, yields, and productivity to increase PHAs' overall cost-effectiveness [302,303]. PHAs can also be compounded, just like the present plastics, to enhance further the material's characteristics [302,303].

Carbon- and metal-based NPs like gold, silver, copper, aluminum, nickel, and cobalt are the most extensively utilized engineered CN. Skin can come into contact with cosmetic items like water- or stain-repellent nano-coated fiber materials, lotions, or creams with nano- TiO_2 or nano-ZnO as sunray protection [304,305]. Additionally, exposure to occupational and environmental hazards occurs naturally due to the production and use of NPs [304,305]. Many reports have implied the toxicity of cell wall damage due to metal oxide NPs including nano-TiO_2, nano-ZnO, nano-CuO, and nano-Fe_2O_3 [306]. Varied materials give rise to different toxicities in NPs. For example, nano-CuO has the highest level of cytotoxicity and damages DNA, causing the creation of 8-hydroxy-20-deoxyguanosine (8-OHdG), whereas nano- TiO_2 has the lowest level of toxicity and produces very little 8-OHdG [306].

Nanomaterials play a direct or indirect impact on genotoxicity by increasing the generation of ROS. DNA strand breakage, crosslinks of DNA proteins, lesions in the base and sugar of DNA, and the development of a primary site are all ROS-induced DNA damage [307]. Antioxidants can be utilized to reduce the damaging effects of ROS [307]. Superoxide dismutases (SODs), peroxidases, and catalases, some of the most potent antioxidants, are utilized to counteract these adverse effects. The transformation of superoxide into the highly reactive hydroxyl radical is a significant factor in many harmful effects of superoxide [307]. Comparing all biological

ROS, this highly reactive hydroxyl radical has the highest one-electron reduction potential. There isn't a prominent enzymatic scavenging mechanism in the body that can eliminate hydroxyl radicals. Antioxidants are the only protection against hydroxyl radicals [308–311]. Chemicals exposed to radiation may result in the production of ROS, which then causes lipid peroxidation. Tumor cells produce more ROS and endure oxidative stress than normal cells do, which promotes mutations, genetic changes, cell expansion, and cell death. Chemicals that forage ROS are, therefore likely candidates for use as tumor therapies [308–311].

The existing protocol for toxicity evaluation possesses several drawbacks as well. For a precise understanding of nanotoxicity, a long-term comprehensive toxicity evaluation is required. Additionally, varied particle compositions used in various research produce inconsistent and dubious results. Therefore, before being used in clinical settings, NPs should be thoroughly described concerning their toxicity, for which it's crucial to understand how biological systems interact with nanomaterials.

10. Challenges and future perspective

Incorporating NPs with antimicrobial properties requires surface chemical modification and specific synthetic routes. Therefore, selection of a synthetic method plays a decisive role in achieving the specific surface properties of NPs (size, shape, and charges). Interestingly, small-sized NPs show better cell penetration attributed to their higher surface-to-volume ratio. The morphology of NPs, such as spherical, triangular, or pyramidal, nano-rods flower shaped, tetrahedral, nano-prism, and nano-bars, highly influence the antibacterial activity and could be exploited to target specific bacteria [312–316]. The surface charge affects the zeta potential of NPs, while influencing the electrostatic attraction between the NPs and the bacterial cells. The negatively charged NPs show repulsion, which hampered their antimicrobial activity. NPs are known to form aggregates due to surface charge and zeta potential, increasing aggregation size and cell penetrability while increasing toxicity. For example, the extracellular chemicals produced by *E. coli* change the size and zeta potential of AgNPs, causing agglomeration and resistance to Ag-NPs [317].

Still, the delivery of NPs to target intracellular bacterial infections in humans is limited due to their local and systemic toxicity [318]. NPs and their breakdown products cause hemolysis, altering blood circulation routes. Larger NPs are more toxic to biological systems than smaller ones [319]. CuO-NPs, ZnO-NPs, and TiO_2-NPs are usually restricted due to oxidative reactions and DNA damage, whereas CuO-NPs may specifically cause hepatotoxicity and nephrotoxicity by interacting with cell components [283,320]. Nanomaterials given intravenously have the potential to accumulate in many organs throughout the body. Hence, toxicity assessment at the cellular and systemic levels is critical because it has a high clinical significance. Thus, the elimination of the nanomaterials is essential after their antimicrobial activity as the clearance of NPs from the body is poor, thus collectively causing toxicity. A few NPs can be eliminated by the kidney, while others that are not destroyed are kept in the body [321]. The poor bioavailability and biodistribution show an adverse effect on the antimicrobial efficacy of the NPs. Moreover, the concerned dosage of nanomaterials for efficient antimicrobial activity is no doubt a matter of concern. Thus, dosage evaluation and optimization are essential to reduce toxicity and enhance the effect of the antimicrobial property of NPs [322,323].

Another shortcoming of existing studies on the antibacterial activities of NPs is the absence of coherent standards. Aberrant microbial strains, NP parameters, and response periods were evaluated in different research, making the comparison of antibacterial efficacy challenging [324]. The most significant challenges connected with the clinical applications of nanomaterials include safety, biocompatibility with the host, biological issues, intellectual property, laws/regulations, time, and cost-effectiveness. As a result, there is a long road ahead before using nanomaterials in clinical trials and therapeutics to combat AMR.

In our understanding, multiple nanomaterials have potential to prevent microbial resistance development. Both preclinical and clinical studies are now being conducted better to grasp the limitations and prospects of various NPs to comprehend their antibacterial characteristics. Nanomaterials, as opposed to antibiotics, are associated with many cellular mechanisms due to their potential utility against antibiotic-resistant bacterial strains. Furthermore, NPs provide several possibilities for the prevention, detection, and treatment of infectious diseases, as well as biofilm management. However, significant research on these nanomaterials is required to understand and assess their impact on humans and the environment before wide-scale commercial usage. The advancement of nanotechnology and nano-theranostics has opened the door for alternative approaches toward novel antibacterial therapeutics, which will revolutionize the field of microbiology, both in the laboratory and on a commercial basis.

11. Conclusion

In summary, this article has discussed various novel nano-based strategies that can be utilized against MDR bacteria. The implication of these strategies on the host immune system. We have presented the immune sensitive of these NPs and nano-based strategies against the adaptive and innate immune systems while focusing on the context of the responses to living microorganisms. Nanomaterials are known to interfere with growth, death, bacteria life cycle, and biofilm formation. NPs interact with various immune system cells to initiate an immune response, and NPs constituting mast cell granules are used to boost immunity during vaccination. The anti-fouling surface of NPs hinders bacterial adhesion and therefore inhibits bacterial infection. We have also discussed the physiological factors that affect the NPs-based strategies against AMR bacteria. Size, shape, zeta potential, optical properties, biocompatibility, surface topology, and steric repulsions are the extensively studies physiological factors which determine the functionality and antimicrobial activity of potentially targeted nanomaterials. The size determines the number of NPs capable of coating the cell surface or the extent to which NPs will penetrate the bacterial cell wall and the shape determines the mechanism of entry. The zeta potential determines whether a particular NP could be used as a therapeutic carrier for enhancing bacterial permeability to cause anti-microbial activity and its influence over the pharmacokinetic behavior of NPs since pH variations modify the charge of the NPs. All commercially available antimicrobial agents are chemically synthesized or naturally extracted. We try to focus on the synthesis, and

surface modification of NPs and nano-conjugated antibiotics and highlighted their pre-clinical investigations. Herein, we have established a foundation for some novel therapies that will pave a new era for nano-strategic-based anti-bacterial therapies highlighting their clinical significance and their impact on immune systems. These novel nano-strategies would include nano-antibiotics, nano-camouflaging, nanorobots, nano-machines, and nanomaterials. We have also illustrated the materials' chemistry and factors modulating the nano theranostics approaches.

Declaration of Competing Interest

None.

Author agreement statement

We the undersigned declare that this manuscript is original, has not been published before and is not currently being considered for publication else where.

We confirm that the manuscript has been read and approved by all named authors and that there are no other persons who satisfied the criteria for authorship but are not listed. We further confirm that the order of authors listed in the manuscript has been approved by all of us.

We understand that the Corresponding Author is the sole contact for the Editorial process. He/she is responsible for communicating with the other authors about progress, submissions of revisions and final approval of proofs.

Authors contribution

The manuscript was conceptualized and written by RB, BB, AN and NKJ. TD, SP, LK, SK, SM, AD, SKJ, SO, KK, and NKJ collected the information and analyzed it. AN, PM, SSD, DI, MK, FA and ACPS helped in revision. All authors participated in editing, writing, revision and proofread. RB, NKJ, SK and AN worked on the illustrations.

Acknowledgement

The authors acknowledge respective departments and institutions for providing facilities and support. The author would like to thank the Deanship of Scientific Research at Majmaah University for supporting this work. We would like to acknowledge BioRender (BioRender.com) for the illustrations.

References

[1] C. Manyi-Loh, et al., Antibiotic use in agriculture and its consequential resistance in environmental sources: potential public health implications, Molecules 23 (4) (2018) 795.
[2] R.O. Darouiche, Treatment of infections associated with surgical implants, N. Engl. J. Med. 350 (14) (2004) 1422–1429.
[3] K.G. Neoh, et al., Surface modification strategies for combating catheter-related complications: recent advances and challenges, J. Mater. Chem. B 5 (11) (2017) 2045–2067.
[4] S. Kimura, Y. Nakamura, Poor Quality Pharmaceuticals in Global Public Health, Springer, 2020.
[5] M.S. Khan, et al., Is enhancing the professionalism of healthcare providers critical to tackling antimicrobial resistance in low-and middle-income countries? Hum. Resour. Health 18 (1) (2020) 1–9.
[6] S.E. Edwards, et al., Combatting antibiotic resistance together: how can we enlist the help of industry? Antibiotics 7 (4) (2018) 111.
[7] C.M. Morel, et al., Industry incentives and antibiotic resistance: an introduction to the antibiotic susceptibility bonus, J. Antibiot. 73 (7) (2020) 421–428.
[8] A. Negi, K.K. Kesari, Chitosan nanoparticle encapsulation of antibacterial essential oils, Micromachines 13 (8) (2022) 1265.
[9] S.A. Alali, et al., Community hospital stethoscope cleaning practices and contamination rates, Am. J. Infect. Control 48 (11) (2020) 1365–1369.
[10] A. Langdon, N. Crook, G. Dantas, The effects of antibiotics on the microbiome throughout development and alternative approaches for therapeutic modulation, Genome Med. 8 (1) (2016) 39.
[11] A. Nath, et al., Phage delivered CRISPR-Cas system to combat multidrug-resistant pathogens in gut microbiome, Biomed. Pharmacother. 151 (2022), 113122.
[12] M.S. Mulani, et al., Emerging strategies to combat ESKAPE pathogens in the era of antimicrobial resistance: a review, Front. Microbiol. 10 (539) (2019).
[13] J.M. Munita, C.A. Arias, Mechanisms of antibiotic resistance, Microbiol. Spectr. 4 (2) (2016).
[14] Intorre, L., La resistenza microbica ai chemioterapici. 2009.
[15] K. Poole, Mechanisms of bacterial biocide and antibiotic resistance, J. Appl. Microbiol. 92 (2002) 55S–64S.
[16] D. Lim, N.C. Strynadka, Structural basis for the β lactam resistance of PBP2a from methicillin-resistant Staphylococcus aureus, Nat. Struct. Biol. 9 (11) (2002) 870–876.
[17] R. Bhattacharjee, et al., Synergy of nanocarriers with CRISPR-Cas9 in an emerging technology platform for biomedical appliances: current insights and perspectives, Mater. Des. 224 (2022), 111415.
[18] R. Bhattacharjee, et al., Theragnostic application of nanoparticle and CRISPR against food-borne multi-drug resistant pathogens, Mater. Today Bio 15 (2022), 100291.
[19] A. Staroń, O. Długosz, Antimicrobial properties of nanoparticles in the context of advantages and potential risks of their use, J. Environ. Sci. Health, Part A (2021) 1–14.
[20] A. Gupta, R.F. Landis, V.M. Rotello, Nanoparticle-based antimicrobials: surface functionality is critical, F1000Research 5 (2016).
[21] R. Bhattacharjee, et al., State-of-art high-performance Nano-systems for mutated coronavirus infection management: from lab to clinic, OpenNano 8 (2022), 100078.
[22] K. Giri, et al., Targeting bacterial biofilms via surface engineering of gold nanoparticles, RSC Adv. 5 (128) (2015) 105551–105559.
[23] R. Bhattacharjee, et al., The emergence of metal oxide nanoparticles (NPs) as a phytomedicine: a two-facet role in plant growth, nano-toxicity and anti-phytomicrobial activity, Biomed. Pharmacother. 155 (2022), 113658.
[24] W.-W. Lin, M. Karin, A cytokine-mediated link between innate immunity, inflammation, and cancer, J. Clin. Invest. 117 (5) (2007) 1175–1183.
[25] J. Scheller, et al., The pro-and anti-inflammatory properties of the cytokine interleukin-6, Biochim. Biophys. Acta 1813 (5) (2011) 878–888.

[26] M.A. Dobrovolskaia, S.E. McNeil, Immunological properties of engineered nanomaterials, Nanosci. Technol.: Collect. Rev. Nat. J. (2010) 278–287.
[27] M.A. Dobrovolskaia, et al., Preclinical studies to understand nanoparticle interaction with the immune system and its potential effects on nanoparticle biodistribution, Mol. Pharmaceutics 5 (4) (2008) 487–495.
[28] T. Kawai, S. Akira, The role of pattern-recognition receptors in innate immunity: update on Toll-like receptors, Nat. Immunol. 11 (5) (2010) 373–384.
[29] M. Schmidt, et al., Crucial role for human Toll-like receptor 4 in the development of contact allergy to nickel, Nat. Immunol. 11 (9) (2010) 814–819.
[30] M. Lucarelli, et al., Innate defence functions of macrophages can be biased by nano-sized ceramic and metallic particles, Eur. Cytokine Netw. 15 (4) (2004) 339–346.
[31] Y. Cui, et al., Signaling pathway of inflammatory responses in the mouse liver caused by TiO2 nanoparticles, J. Biomed. Mater. Res. Part A 96 (1) (2011) 221–229.
[32] Castillo, P.M., et al., Tiopronin monolayer-protected silver nanoparticles modulate IL-6 secretion mediated by Toll-like receptor ligands. 2008.
[33] H. Chang, et al., Involvement of MyD88 in zinc oxide nanoparticle-induced lung inflammation, Exp. Toxicol. Pathol. 65 (6) (2013) 887–896.
[34] C.-C. Ho, et al., Quantum dots induced monocyte chemotactic protein-1 expression via MyD88-dependent Toll-like receptor signaling pathways in macrophages, Toxicology 308 (2013) 1–9.
[35] P. Chen, K. Kanehira, A. Taniguchi, Role of toll-like receptors 3, 4 and 7 in cellular uptake and response to titanium dioxide nanoparticles, Sci. Technol. Adv. Mater. (2013).
[36] C. Dostert, et al., Innate immune activation through Nalp3 inflammasome sensing of asbestos and silica, Science 320 (5876) (2008) 674–677.
[37] V. Hornung, et al., Silica crystals and aluminum salts activate the NALP3 inflammasome through phagosomal destabilization, Nat. Immunol. 9 (8) (2008) 847–856.
[38] S.L. Cassel, et al., The Nalp3 inflammasome is essential for the development of silicosis, Proc. Natl Acad. Sci. 105 (26) (2008) 9035–9040.
[39] S.C. Eisenbarth, et al., Crucial role for the Nalp3 inflammasome in the immunostimulatory properties of aluminium adjuvants, Nature 453 (7198) (2008) 1122–1126.
[40] B. Sun, et al., NLRP3 inflammasome activation induced by engineered nanomaterials, Small 9 (9-10) (2013) 1595–1607.
[41] R. Muñoz-Planillo, et al., K+ efflux is the common trigger of NLRP3 inflammasome activation by bacterial toxins and particulate matter, Immunity 38 (6) (2013) 1142–1153.
[42] A.C. Reisetter, et al., Induction of inflammasome-dependent pyroptosis by carbon black nanoparticles, J. Biol. Chem. 286 (24) (2011) 21844–21852.
[43] F.T. Andón, et al., Hollow carbon spheres trigger inflammasome-dependent IL-1β secretion in macrophages, Carbon 113 (2017) 243–251.
[44] P. Italiani, D. Boraschi, From monocytes to M1/M2 macrophages: phenotypical vs. functional differentiation, Front. Immunol. 5 (2014) 514.
[45] T.A. Wynn, A. Chawla, J.W. Pollard, Macrophage biology in development, homeostasis and disease, Nature 496 (7446) (2013) 445–455.
[46] S. Gordon, A. Plüddemann, F.Martinez Estrada, Macrophage heterogeneity in tissues: phenotypic diversity and functions, Immunol. Rev. 262 (1) (2014) 36–55.
[47] F.O. Martinez, Regulators of macrophage activation, Eur. J. Immunol. 41 (6) (2011) 1531–1534.
[48] A. Mantovani, et al., Macrophage polarization: tumor-associated macrophages as a paradigm for polarized M2 mononuclear phagocytes, Trends Immunol. 23 (11) (2002) 549–555.
[49] J. Hoppstädter, et al., M2 polarization enhances silica nanoparticle uptake by macrophages, Front. Pharmacol. 6 (2015) 55.
[50] X. Miao, X. Leng, Q. Zhang, The current state of nanoparticle-induced macrophage polarization and reprogramming research, Int. J. Mol. Sci. 18 (2) (2017) 336.
[51] H.J. Yen, S.h. Hsu, C.L. Tsai, Cytotoxicity and immunological response of gold and silver nanoparticles of different sizes, Small 5 (13) (2009) 1553–1561.
[52] M. Giovanni, et al., Pro-inflammatory responses of RAW264. 7 macrophages when treated with ultralow concentrations of silver, titanium dioxide, and zinc oxide nanoparticles, J. Hazard. Mater. 297 (2015) 146–152.
[53] J. Ma, et al., Crucial role of lateral size for graphene oxide in activating macrophages and stimulating pro-inflammatory responses in cells and animals, ACS Nano 9 (10) (2015) 10498–10515.
[54] R. Weissleder, M. Nahrendorf, M.J. Pittet, Imaging macrophages with nanoparticles, Nat. Mater. 13 (2) (2014) 125–138.
[55] Y. Li, et al., Near-infrared light triggered phototherapy and immunotherapy for elimination of methicillin-resistant Staphylococcus aureus biofilm infection on bone implant, ACS Nano 14 (7) (2020) 8157–8170.
[56] G. Guo, et al., Space-selective chemodynamic therapy of CuFe5O8 nanocubes for implant-related infections, ACS Nano 14 (10) (2020) 13391–13405.
[57] J. Wang, et al., Magneto-based synergetic therapy for implant-associated infections via biofilm disruption and innate immunity regulation, Adv. Sci. 8 (6) (2021), 2004010.
[58] M. Bartneck, et al., Phagocytosis independent extracellular nanoparticle clearance by human immune cells, Nano Lett. 10 (1) (2010) 59–63.
[59] V. Brinkmann, A. Zychlinsky, Neutrophil extracellular traps: is immunity the second function of chromatin? J. Cell Biol. 198 (5) (2012) 773–783.
[60] Z. Wang, et al., Prevention of vascular inflammation by nanoparticle targeting of adherent neutrophils, Nat. Nanotechnol. 9 (3) (2014) 204–210.
[61] E.Y. Chen, et al., A mixture of anatase and rutile TiO 2 nanoparticles induces histamine secretion in mast cells, Part. Fibre Toxicol. 9 (1) (2012) 1–10.
[62] A.L.S. John, et al., Synthetic mast-cell granules as adjuvants to promote and polarize immunity in lymph nodes, Nat. Mater. 11 (3) (2012) 250–257.
[63] B.C. Schanen, et al., Exposure to titanium dioxide nanomaterials provokes inflammation of an in vitro human immune construct, ACS Nano 3 (9) (2009) 2523–2532.
[64] Y. Liu, et al., The effect of Gd@ C82 (OH) 22 nanoparticles on the release of Th1/Th2 cytokines and induction of TNF-α mediated cellular immunity, Biomaterials 30 (23-24) (2009) 3934–3945.
[65] S. Tomić, et al., Size-dependent effects of gold nanoparticles uptake on maturation and antitumor functions of human dendritic cells in vitro, PLoS One 9 (5) (2014) e96584.
[66] P.L. Mottram, et al., Type 1 and 2 immunity following vaccination is influenced by nanoparticle size: formulation of a model vaccine for respiratory syncytial virus, Mol. Pharmaceutics 4 (1) (2007) 73–84.
[67] T. Storni, et al., Immunity in response to particulate antigen-delivery systems, Adv. Drug. Deliv. Rev. 57 (3) (2005) 333–355.
[68] V.V. Temchura, et al., Targeting and activation of antigen-specific B-cells by calcium phosphate nanoparticles loaded with protein antigen, Biomaterials 35 (23) (2014) 6098–6105.
[69] C.-C. Shen, et al., A single exposure to iron oxide nanoparticles attenuates antigen-specific antibody production and T-cell reactivity in ovalbumin-sensitized BALB/c mice, Int. J. Nanomed. 6 (2011) 1229.
[70] H. Tang, et al., Photosensitizer nanodot eliciting immunogenicity for photo-immunologic therapy of postoperative methicillin-resistant Staphylococcus aureus infection and secondary recurrence, Adv. Mater. 34 (12) (2022), 2107300.
[71] P. Zhang, et al., Fe3O4@ TiO2-Laden neutrophils activate innate immunity via photosensitive reactive oxygen species release, Nano Lett. 20 (1) (2019) 261–271.
[72] D. Campoccia, L. Montanaro, C.R. Arciola, A review of the biomaterials technologies for infection-resistant surfaces, Biomaterials 34 (34) (2013) 8533–8554.
[73] J.R. Morones, et al., The bactericidal effect of silver nanoparticles, Nanotechnology 16 (10) (2005) 2346.
[74] Y.-H. Hsueh, et al., The antimicrobial properties of silver nanoparticles in Bacillus subtilis are mediated by released Ag+ ions, PLoS One 10 (12) (2015), e0144306.
[75] P. Bagga, et al., Gold nanoparticles conjugated levofloxacin: for improved antibacterial activity over levofloxacin alone, Curr. Drug Delivery 14 (8) (2017) 1114–1119.
[76] T. Mironava, et al., Gold nanoparticles cellular toxicity and recovery: effect of size, concentration and exposure time, Nanotoxicology 4 (1) (2010) 120–137.
[77] B. Sadeghi, et al., Comparison of the anti-bacterial activity on the nanosilver shapes: nanoparticles, nanorods and nanoplates, Adv. Powder Technol. 23 (1) (2012) 22–26.
[78] T. Ahmad, et al., Biosynthesis, structural characterization and antimicrobial activity of gold and silver nanoparticles, Colloids Surf. B 107 (2013) 227–234.
[79] I.A. Wani, T. Ahmad, Size and shape dependant antifungal activity of gold nanoparticles: a case study of Candida, Colloids Surf. B 101 (2013) 162–170.

[80] I. Sondi, B. Salopek-Sondi, Silver nanoparticles as antimicrobial agent: a case study on E. coli as a model for Gram-negative bacteria, J. Colloid Interface Sci. 275 (1) (2004) 177–182.
[81] L. Kvítek, et al., Effect of surfactants and polymers on stability and antibacterial activity of silver nanoparticles (NPs), J. Phys. Chem. C 112 (15) (2008) 5825–5834.
[82] D.F. Moyano, et al., Nanoparticle hydrophobicity dictates immune response, J. Am. Chem. Soc. 134 (9) (2012) 3965–3967.
[83] V. Ayala, et al., Effect of surface charge on the colloidal stability and in vitro uptake of carboxymethyl dextran-coated iron oxide nanoparticles, J. Nanopart. Res. 15 (8) (2013) 1–14.
[84] M. Meléndrez, G. Cárdenas, J. Arbiol, Synthesis and characterization of gallium colloidal nanoparticles, J. Colloid Interface Sci. 346 (2) (2010) 279–287.
[85] K.H. Jacobson, et al., Lipopolysaccharide density and structure govern the extent and distance of nanoparticle interaction with actual and model bacterial outer membranes, Environ. Sci. Technol. 49 (17) (2015) 10642–10650.
[86] D.S. Snyder, T.J. McIntosh, The lipopolysaccharide barrier: correlation of antibiotic susceptibility with antibiotic permeability and fluorescent probe binding kinetics, Biochemistry 39 (38) (2000) 11777–11787.
[87] S. Halder, et al., Alteration of Zeta potential and membrane permeability in bacteria: a study with cationic agents, SpringerPlus 4 (1) (2015) 1–14.
[88] M.S. Khan, et al., Highly efficient gold nanorods assisted laser phototherapy for rapid treatment on mice wound infected by pathogenic bacteria, J. Ind. Eng. Chem. 36 (2016) 49–58.
[89] N.J. Millenbaugh, et al., Photothermal killing of Staphylococcus aureus using antibody-targeted gold nanoparticles, Int. J. Nanomed. 10 (2015) 1953.
[90] D.K. Kirui, et al., Targeted laser therapy synergistically enhances efficacy of antibiotics against multi-drug resistant Staphylococcus aureus and Pseudomonas aeruginosa biofilms, Nanomed. Nanotechnol. Biol. Med. 20 (2019), 102018.
[91] D.D Evanoff Jr, G. Chumanov, Synthesis and optical properties of silver nanoparticles and arrays, ChemPhysChem 6 (7) (2005) 1221–1231.
[92] C. Jayaseelan, et al., Novel microbial route to synthesize ZnO nanoparticles using Aeromonas hydrophila and their activity against pathogenic bacteria and fungi, Spectrochim. Acta Part A 90 (2012) 78–84.
[93] K.M. Mayer, J.H. Hafner, Localized surface plasmon resonance sensors, Chem. Rev. 111 (6) (2011) 3828–3857.
[94] K.L. Kelly, et al., The Optical Properties of Metal Nanoparticles: the Influence of Size, Shape, and Dielectric Environment, ACS Publications, 2003, pp. 668–677.
[95] F. Vatansever, et al., Antimicrobial strategies centered around reactive oxygen species–bactericidal antibiotics, photodynamic therapy, and beyond, FEMS Microbiol. Rev. 37 (6) (2013) 955–989.
[96] Y. Zhang, et al., Plasmonic engineering of singlet oxygen generation, Proc. Natl Acad. Sci. 105 (6) (2008) 1798–1802.
[97] L.S. de Melo, et al., Singlet oxygen generation enhanced by silver-pectin nanoparticles, J. Fluoresc. 22 (6) (2012) 1633–1638.
[98] M. Dong, et al., Red-shifting azobenzene photoswitches for in vivo use, Acc. Chem. Res. 48 (10) (2015) 2662–2670.
[99] A. Negi, C. Kieffer, A.S. Voisin-Chiret, Azobenzene photoswitches in proteolysis targeting chimeras: photochemical control strategies and therapeutic benefits, ChemistrySelect 7 (23) (2022), e202200981.
[100] A.A. Beharry, G.A. Woolley, Azobenzene photoswitches for biomolecules, Chem. Soc. Rev. 40 (8) (2011) 4422–4437.
[101] A. Negi, K.K. Kesari, A.S. Voisin-Chiret, Light-activating PROTACs in cancer: chemical design, challenges, and applications, Appl. Sci. 12 (19) (2022) 9674.
[102] S. Khan, et al., Gold nanoparticles enhance methylene blue–induced photodynamic therapy: a novel therapeutic approach to inhibit Candida albicans biofilm, Int. J. Nanomed. 7 (2012) 3245–3257.
[103] M.A. Sherwani, et al., Gold nanoparticle-photosensitizer conjugate based photodynamic inactivation of biofilm producing cells: potential for treatment of C. albicans infection in BALB/c mice, PLoS One 10 (7) (2015), e0131684.
[104] R. Jijie, et al., Particle-based photodynamic therapy based on indocyanine green modified plasmonic nanostructures for inactivation of a Crohn's disease-associated Escherichia coli strain, J. Mater. Chem. B 4 (15) (2016) 2598–2605.
[105] N. Nombona, et al., Synthesis, photophysics and photochemistry of phthalocyanine-ε-polylysine conjugates in the presence of metal nanoparticles against Staphylococcus aureus, J. Photochem. Photobiol. A 233 (2012) 24–33.
[106] C.S. Seney, B.M. Gutzman, R.H. Goddard, Correlation of size and surface-enhanced Raman scattering activity of optical and spectroscopic properties for silver nanoparticles, J. Phys. Chem. C 113 (1) (2009) 74–80.
[107] S. Hong, X. Li, Optimal size of gold nanoparticles for surface-enhanced Raman spectroscopy under different conditions, J. Nanomater. 2013 (2013).
[108] M.S. Ribeiro, et al., Photodynamic inactivation assisted by localized surface plasmon resonance of silver nanoparticles: In vitro evaluation on Escherichia coli and Streptococcus mutans, Photodiagn. Photodyn. Ther. 22 (2018) 191–196.
[109] W.P. Hammes, F.C. Neuhaus, On the mechanism of action of vancomycin: inhibition of peptidoglycan synthesis in Gaffkya homari, Antimicrob. Agents Chemother. 6 (6) (1974) 722–728.
[110] C. Marshall, et al., D-Ala-D-Ala ligases from glycopeptide antibiotic-producing organisms are highly homologous to the enterococcal vancomycin-resistance ligases VanA and VanB, Proc. Natl Acad. Sci. 94 (12) (1997) 6480–6483.
[111] D. Hughes, Exploiting genomics, genetics and chemistry to combat antibiotic resistance, Nat. Rev. Genet. 4 (6) (2003) 432–441.
[112] S.M. Abdelghany, et al., Gentamicin-loaded nanoparticles show improved antimicrobial effects towards Pseudomonas aeruginosa infection, Int. J. Nanomed. 7 (2012) 4053.
[113] J. Davies, Where have all the antibiotics gone? Canadian J. Infect. Dis. Med. Microbiol. 17 (5) (2006) 287–290.
[114] G. Devasahayam, W.M. Scheld, P.S. Hoffman, Newer antibacterial drugs for a new century, Expert Opin. Investig. Drugs 19 (2) (2010) 215–234.
[115] E. Power, Impact of antibiotic restrictions: the pharmaceutical perspective, Clin. Microbiol. Infect. 12 (2006) 25–34.
[116] D. Biedenbach, et al., In vitro activity of gepotidacin, a novel triazaacenaphthylene bacterial topoisomerase inhibitor, against a broad spectrum of bacterial pathogens, Antimicrob. Agents Chemother. 60 (3) (2016) 1918–1923.
[117] W.H. Organization, Antibacterial Agents in Clinical Development: An Analysis of the Antibacterial Clinical Development Pipeline, Including Tuberculosis, World Health Organization, 2017.
[118] A. Rodzinski, et al., Targeted and controlled anticancer drug delivery and release with magnetoelectric nanoparticles, Sci. Rep. 6 (1) (2016) 1–14.
[119] N. Cassir, J.-M. Rolain, P. Brouqui, A new strategy to fight antimicrobial resistance: the revival of old antibiotics, Front. Microbiol. 5 (2014) 551.
[120] P. Khadka, et al., Pharmaceutical particle technologies: an approach to improve drug solubility, dissolution and bioavailability, Asian J. Pharm. Sci. 9 (6) (2014) 304–316.
[121] G.D. Bixler, et al., Anti-fouling properties of microstructured surfaces bio-inspired by rice leaves and butterfly wings, J. Colloid Interface Sci. 419 (2014) 114–133.
[122] N. Murthy, et al., Self-assembled and etched cones on laser ablated polymer surfaces, J. Appl. Phys. 100 (2006), 023538.
[123] S. Nishimoto, B. Bhushan, Bioinspired self-cleaning surfaces with superhydrophobicity, superoleophobicity, and superhydrophilicity, RSC Adv. 3 (3) (2013) 671–690.
[124] S. Krishnan, C.J. Weinman, C.K. Ober, Advances in polymers for anti-biofouling surfaces, J. Mater. Chem. 18 (29) (2008) 3405–3413.
[125] L.H. Evers, D. Bhavsar, P. Mailänder, The biology of burn injury, Exp. Dermatol. 19 (9) (2010) 777–783.
[126] J.B. Schlenoff, Zwitteration: coating surfaces with zwitterionic functionality to reduce nonspecific adsorption, Langmuir 30 (32) (2014) 9625–9636.
[127] J. Hasan, R.J. Crawford, E.P. Ivanova, Antibacterial surfaces: the quest for a new generation of biomaterials, Trends Biotechnol. 31 (5) (2013) 295–304.
[128] J.C. Hower, et al., Hydration of "nonfouling" functional groups, J. Phys. Chem. B 113 (1) (2009) 197–201.
[129] R.H. Brown, et al., Electrospinning zwitterion-containing nanoscale acrylic fibers, Polymer 50 (20) (2009) 4781–4787.
[130] R. Lalani, L. Liu, Synthesis, characterization, and electrospinning of zwitterionic poly (sulfobetaine methacrylate), Polymer 52 (23) (2011) 5344–5354.
[131] S.-H. Ye, et al., Nonthrombogenic, biodegradable elastomeric polyurethanes with variable sulfobetaine content, ACS Appl. Mater. Interfaces 6 (24) (2014) 22796–22806.
[132] S. He, et al., 2D AuPd alloy nanosheets: one-step synthesis as imaging-guided photonic nano-antibiotics, Nanoscale Adv. 2 (8) (2020) 3550–3560.
[133] Fernando, S., T. Gunasekara, and J. Holton, Antimicrobial nanoparticles: applications and mechanisms of action. 2018.

[134] W. Stöber, A. Fink, E. Bohn, Controlled growth of monodisperse silica spheres in the micron size range, J. Colloid Interface Sci. 26 (1) (1968) 62–69.
[135] K.S. Rao, et al., A novel method for synthesis of silica nanoparticles, J. Colloid Interface Sci. 289 (1) (2005) 125–131.
[136] U. Zulfiqar, T. Subhani, S.W. Husain, Synthesis and characterization of silica nanoparticles from clay, J. Asian Ceram. Soc. 4 (1) (2016) 91–96.
[137] U. Zulfiqar, T. Subhani, S.Wilayat Husain, Synthesis of silica nanoparticles from sodium silicate under alkaline conditions, J. Sol-Gel Sci. Technol. 77 (3) (2016) 753–758.
[138] S. Sterman, J.G. Marsden, Silane coupling agents, Ind. Eng. Chem. 58 (3) (1966) 33–37.
[139] F.J. Arriagada, K. Osseo-Asare, Synthesis of nanosize silica in aerosol OT reverse microemulsions, J. Colloid Interface Sci. 170 (1) (1995) 8–17.
[140] M.A. López-Quintela, Synthesis of nanomaterials in microemulsions: formation mechanisms and growth control, Curr. Opin. Colloid Interface Sci. 8 (2) (2003) 137–144.
[141] Y.-S. Cho, Fabrication of hollow or macroporous silica particles by spray drying of colloidal dispersion, J. Dispersion Sci. Technol. 37 (1) (2016) 23–33.
[142] F. Yan, et al., Synthesis and characterization of silica nanoparticles preparing by low-temperature vapor-phase hydrolysis of SiCl4, Ind. Eng. Chem. Res. 53 (30) (2014) 11884–11890.
[143] X. Cai, et al., Synthesis of silica powders by pressured carbonation, Chem. Eng. J. 151 (1) (2009) 380–386.
[144] Y. Bao, et al., Micelle-template synthesis of hollow silica spheres for improving water vapor permeability of waterborne polyurethane membrane, Sci. Rep. 7 (1) (2017) 46638.
[145] L. Xiong, et al., Magnetic core–shell silica nanoparticles with large radial mesopores for siRNA delivery, Small 12 (34) (2016) 4735–4742.
[146] I. Makarovsky, et al., Novel triclosan-bound hybrid-silica nanoparticles and their enhanced antimicrobial properties, Adv. Funct. Mater. 21 (22) (2011) 4295–4304.
[147] G. Qi, et al., Vancomycin-modified mesoporous silica nanoparticles for selective recognition and killing of pathogenic gram-positive bacteria over macrophage-like cells, ACS Appl. Mater. Interfaces 21 (5) (2013) 10874–10881.
[148] D. Pedraza, et al., Amine-functionalized mesoporous silica nanoparticles: a new nanoantibiotic for bone infection treatment, Biomed. Glasses 4 (1) (2018) 1–12.
[149] V. Selvarajan, S. Obuobi, P.L.R. Ee, Silica nanoparticles—a versatile tool for the treatment of bacterial infections, Front. Chem. (8) (2020).
[150] V. Selvarajan, S. Obuobi, P.L.R. Ee, Silica nanoparticles—a versatile tool for the treatment of bacterial infections, Front. Chem. 8 (2020) 602.
[151] R. Badar, A.A. Zahid, M. Yar, 11 - Chitin-Based Nanomaterials, Elsevier, 2021, pp. 249–275. Biopolymeric Nanomaterisals, S. Kanwar, et al., Editors.
[152] M.B. Coltelli, et al., Chitin nanofibril-nanolignin complexes as carriers of functional molecules for skin contact applications, Nanomaterials 12 (8) (2022).
[153] M.-C. Li, et al., Chitin nanofibers as reinforcing and antimicrobial agents in carboxymethyl cellulose films: influence of partial deacetylation, ACS Sustain. Chem. Eng. 4 (8) (2016) 4385–4395.
[154] S. Ifuku, H. Saimoto, Chitin nanofibers: preparations, modifications, and applications, Nanoscale 4 (11) (2012) 3308–3318.
[155] I.F. Escapa, et al., Disruption of β-oxidation pathway in Pseudomonas putida KT2442 to produce new functionalized PHAs with thioester groups, Appl. Microbiol. Biotechnol. 89 (5) (2011) 1583–1598.
[156] T. Sjöström, A.H. Nobbs, B. Su, Bactericidal nanospike surfaces via thermal oxidation of Ti alloy substrates, Mater. Lett. 167 (2016) 22–26.
[157] J. Jenkins, et al., Antibacterial effects of nanopillar surfaces are mediated by cell impedance, penetration and induction of oxidative stress, Nat. Commun. 11 (1) (2020) 1626.
[158] D. Carol López de, et al., Antimicrobial effect of titanium dioxide nanoparticles, in: M Mihai (Ed.), Antimicrobial Resistance, IntechOpen: Rijeka, 2020 et al., Editorsp. Ch. 5.
[159] C.-I. Cheigh, et al., Comparison of intense pulsed light-and ultraviolet (UVC)-induced cell damage in Listeria monocytogenes and Escherichia coli O157: H7, Food Control 25 (2) (2012) 654–659.
[160] R. Van Grieken, et al., Comparison between the photocatalytic inactivation of Gram-positive E. faecalis and Gram-negative E. coli faecal contamination indicator microorganisms, Appl. Catal. B 100 (1-2) (2010) 212–220.
[161] N. Kanjanathaworn, et al., Reduction of cytotoxicity of natural rubber latex film by coating with PMMA-chitosan nanoparticles, Carbohydr. Polym. 97 (1) (2013) 52–58.
[162] T. Suteewong, et al., PMMA particles coated with chitosan-silver nanoparticles as a dual antibacterial modifier for natural rubber latex films, Colloids Surf. B 174 (2019) 544–552.
[163] M. Farshbaf, et al., Significant role of cationic polymers in drug delivery systems, Artif. Cells, Nanomed., Biotechnol. 46 (8) (2018) 1872–1891.
[164] R. Du, X. Feng, A. Chakma, Poly(N,N-dimethylaminoethyl methacrylate)/polysulfone composite membranes for gas separations, J. Membr. Sci. 279 (1) (2006) 76–85.
[165] M. Wang, et al., Surface modification of CdSe and CdSe/ZnS semiconductor nanocrystals with Poly(N,N-dimethylaminoethyl methacrylate), Macromolecules 39 (10) (2006) 3664–3672.
[166] Y. Zhang, et al., Design and biophysical characterization of bioresponsive degradable poly(dimethylaminoethyl methacrylate) based polymers for in vitro DNA transfection, Biomacromolecules 13 (2) (2012) 313–322.
[167] V.I. Martín, et al., Host-guest interactions between cyclodextrins and surfactants with functional groups at the end of the hydrophobic tail, J. Colloid Interface Sci. 491 (2017) 336–348.
[168] M.L. Moyá, et al., Preparation and characterization of new liposomes. Bactericidal activity of cefepime encapsulated into cationic liposomes, Pharmaceutics 11 (2) (2019) 69.
[169] D.Y. Wang, et al., Lipid-based antimicrobial delivery-systems for the treatment of bacterial infections, Front. Chem. 7 (2019) 872.
[170] D. Li, et al., Preparation of cefquinome sulfate cationic proliposome and evaluation of its efficacy on Staphylococcus aureus biofilm, Colloids Surf. B 182 (2019), 110323.
[171] B.M. Discher, et al., Cross-linked polymersome membranes: vesicles with broadly adjustable properties, J. Phys. Chem. B 106 (11) (2002) 2848–2854.
[172] Y.-Y. Won, H.T. Davis, F.S. Bates, Giant wormlike rubber micelles, Science 283 (5404) (1999) 960–963.
[173] B.M. Discher, et al., Polymer vesicles in various media, Curr. Opin. Colloid Interface Sci. 5 (1) (2000) 125–131.
[174] E. Porges, et al., Antibiotic-loaded polymersomes for clearance of intracellular Burkholderia thailandensis, ACS Nano 15 (12) (2021) 19284–19297.
[175] K. Wayakanon, et al., Polymersome-mediated intracellular delivery of antibiotics to treat Porphyromonas gingivalis-infected oral epithelial cells, FASEB J. 27 (11) (2013) 4455–4465.
[176] T. Wang, et al., Intelligent design of polymersomes for antibacterial and anticancer applications, WIREs Nanomed. Nanobiotechnol. 14 (5) (2022) e1822.
[177] E. Grotz, et al., Pulmonary delivery of rifampicin-loaded soluplus micelles against Mycobacterium tuberculosis, J. Drug Delivery Sci. Technol. 53 (2019), 101170.
[178] L. Zhou, et al., Correction: a highly antibacterial polymeric hybrid micelle with efficiently targeted anticancer siRNA delivery and anti-infection in vitro/in vivo, Nanoscale 11 (10) (2019), 4614-4614.
[179] M. Saraei, et al., Antibacterial polymeric micelles based on kojic acid/acrylic acid/chitosan, Int. J. Polymer. Mater. Polymer. Biomater. (2022) 1–12.
[180] M.B. Khan, Z.H. Khan, Nanodiamonds: synthesis and applications, Nanomater. Appl. (2018) 1–26.
[181] J. Wehling, et al., Bactericidal activity of partially oxidized nanodiamonds, ACS Nano 8 (6) (2014) 6475–6483.
[182] S. Szunerits, A. Barras, R. Boukherroub, Antibacterial applications of nanodiamonds, Int. J. Environ. Res. Public Health 13 (4) (2016) 413.
[183] M. Khanal, et al., Selective antimicrobial and antibiofilm disrupting properties of functionalized diamond nanoparticles against Escherichia coli and Staphylococcus aureus, Part. Part. Syst. Charact. 32 (8) (2015) 822–830.
[184] A. Cumont, et al., Properties, mechanism and applications of diamond as an antibacterial material, Funct. Diamond 1 (1) (2021) 1–28.
[185] M. Milazzo, et al., Biodegradable polymeric micro/nano-structures with intrinsic antifouling/antimicrobial properties: relevance in damaged skin and other biomedical applications, J. Funct. Biomater. 11 (3) (2020) 60.
[186] J.N. O'Sullivan, et al., Protecting the outside: Biological tools to manipulate the skin microbiota, FEMS Microbiol. Ecol. 96 (6) (2020) fiaa085.

[187] N. Hachicho, et al., Effect of silver nanoparticles and silver ions on growth and adaptive response mechanisms of Pseudomonas putida mt-2, FEMS Microbiol. Lett. 355 (1) (2014) 71–77.
[188] X. Wang, et al., A bactericidal microfluidic device constructed using nano-textured black silicon, RSC Adv. 6 (31) (2016) 26300–26306.
[189] R. Saginur, K.N. Suh, Staphylococcus aureus bacteraemia of unknown primary source: where do we stand? Int. J. Antimicrob. Agents 32 (2008) S21–S25.
[190] S. Enoch, A. Roshan, M. Shah, Emergency and early management of burns and scalds, BMJ (2009) 338.
[191] I.S. Kurtz, J.D. Schiffman, Current and emerging approaches to engineer antibacterial and antifouling electrospun nanofibers, Materials 11 (7) (2018) 1059.
[192] S. Li, et al., Antibacterial hydrogels, Adv. Sci. 5 (5) (2018), 1700527.
[193] A.C. Lima, J.F. Mano, Micro/nano-structured superhydrophobic surfaces in the biomedical field: part II: applications overview, Nanomedicine 10 (2) (2015) 271–297.
[194] J.T. Simpson, S.R. Hunter, T. Aytug, Superhydrophobic materials and coatings: a review, Rep. Prog. Phys. 78 (8) (2015), 086501.
[195] N. Nuraje, et al., Superhydrophobic electrospun nanofibers, J. Mater. Chem. A 1 (6) (2013) 1929–1946.
[196] J.A. Aguilar-Briseño, et al., Sulphated polysaccharides from Ulva clathrata and Cladosiphon okamuranus seaweeds both inhibit viral attachment/entry and cell-cell fusion, NDV Infection. Mar. Drugs 13 (2) (2015) 697–712.
[197] S. Danti, et al., Development of tissue-engineered substitutes of the ear ossicles: PORP-shaped poly (propylene fumarate)-based scaffolds cultured with human mesenchymal stromal cells, J. Biomed. Mater. Res. Part A: Offic. J. Soc. Biomater., Japanese Soc. Biomater., Austr. Soc. Biomater. Korean Soc. Biomater. 92 (4) (2010) 1343–1356.
[198] M.S. Ganewatta, C. Tang, Controlling macromolecular structures towards effective antimicrobial polymers, Polymer 63 (2015) A1–A29.
[199] A.M. Carmona-Ribeiro, L.D. De Melo Carrasco, Cationic antimicrobial polymers and their assemblies, Int. J. Mol. Sci. 14 (5) (2013) 9906–9946.
[200] L. Hall-Stoodley, J.W. Costerton, P. Stoodley, Bacterial biofilms: from the natural environment to infectious diseases, Nat. Rev. Microbiol. 2 (2) (2004) 95–108.
[201] D. Pavithra, M. Doble, Biofilm formation, bacterial adhesion and host response on polymeric implants—issues and prevention, Biomed. Mater. 3 (3) (2008), 034003.
[202] J.L. Harding, M.M. Reynolds, Combating medical device fouling, Trends Biotechnol. 32 (3) (2014) 140–146.
[203] R.E. Hancock, H.-G. Sahl, Antimicrobial and host-defense peptides as new anti-infective therapeutic strategies, Nat. Biotechnol. 24 (12) (2006) 1551–1557.
[204] A. Peschel, H.-G. Sahl, The co-evolution of host cationic antimicrobial peptides and microbial resistance, Nat. Rev. Microbiol. 4 (7) (2006) 529–536.
[205] C.D. Fjell, et al., Designing antimicrobial peptides: form follows function, Nat. Rev. Drug Discovery 11 (1) (2012) 37–51.
[206] M.N. Melo, R. Ferre, M.A. Castanho, Antimicrobial peptides: linking partition, activity and high membrane-bound concentrations, Nat. Rev. Microbiol. 7 (3) (2009) 245–250.
[207] K.A. Brogden, Antimicrobial peptides: pore formers or metabolic inhibitors in bacteria? Nat. Rev. Microbiol. 3 (3) (2005) 238–250.
[208] H. Takahashi, et al., Molecular design, structures, and activity of antimicrobial peptide-M imetic polymers, Macromol. Biosci. 13 (10) (2013) 1285–1299.
[209] W.S. Horne, S.H. Gellman, Foldamers with heterogeneous backbones, Acc. Chem. Res. 41 (10) (2008) 1399–1408.
[210] F.J. Alvarez, The effect of chitin size, shape, source and purification method on immune recognition, Molecules 19 (4) (2014) 4433–4451.
[211] S. Danti, et al., Chitin nanofibrils and nanolignin as functional agents in skin regeneration, Int. J. Mol. Sci. 20 (11) (2019) 2669.
[212] L. Panariello, et al., Chitosan and nano-structured chitin for biobased anti-microbial treatments onto cellulose based materials, Eur. Polym. J. 113 (2019) 328–339.
[213] N. Dinjaski, et al., PHACOS, a functionalized bacterial polyester with bactericidal activity against methicillin-resistant Staphylococcus aureus, Biomaterials 35 (1) (2014) 14–24.
[214] E. Elmowafy, et al., Polyhydroxyalkanoate (PHA): applications in drug delivery and tissue engineering, Expert Rev. Med. Devices 16 (6) (2019) 467–482.
[215] R. Rai, et al., Highly elastomeric poly (3-hydroxyoctanoate) based natural polymer composite for enhanced keratinocyte regeneration, Int. J. Polymer. Mater. Polymer. Biomater. 66 (7) (2017) 326–335.
[216] T. Keshavarz, I. Roy, Polyhydroxyalkanoates: bioplastics with a green agenda, Curr. Opin. Microbiol. 13 (3) (2010) 321–326.
[217] S.J. Kim, et al., The potential role of polymethyl methacrylate as a new packaging material for the implantable medical device in the bladder, Biomed. Res. Int. 2015 (2015).
[218] V. Tzankova, et al., In vitro and in vivo toxicity evaluation of cationic PDMAEMA-PCL-PDMAEMA micelles as a carrier of curcumin, Food Chem. Toxicol. 97 (2016) 1–10.
[219] A. Gonzalez Gomez, et al., Liposomal nanovesicles for efficient encapsulation of Staphylococcal antibiotics, ACS Omega 4 (6) (2019) 10866–10876.
[220] P. Walvekar, et al., Self-assembled oleylamine grafted hyaluronic acid polymersomes for delivery of vancomycin against methicillin resistant Staphylococcus aureus (MRSA), Colloids Surf. B 182 (2019), 110388.
[221] J.S. Lee, J. Feijen, Polymersomes for drug delivery: design, formation and characterization, J. Controlled Release 161 (2) (2012) 473–483.
[222] P.J. Photos, et al., Polymer vesicles in vivo: correlations with PEG molecular weight, J. Controlled Release 90 (3) (2003) 323–334.
[223] V. Awasthi, et al., Neutral and anionic liposome-encapsulated hemoglobin: effect of postinserted poly (ethylene glycol)-distearoylphosphatidylethanolamine on distribution and circulation kinetics, J. Pharmacol. Exp. Ther. 309 (1) (2004) 241–248.
[224] F. Meng, et al., Pegylated polystyrene particles as a model system for artificial cells, J. Biomed. Mater. Res. Part A: Offic. J. Soc. Biomater., Japanese Soc. Biomater., Austr. Soc. Biomater. Korean Soc. Biomater. 70 (1) (2004) 97–106.
[225] M.C. Woodle, Surface-modified liposomes: assessment and characterization for increased stability and prolonged blood circulation, Chem. Phys. Lipids. 64 (1) (1993) 249–262.
[226] K. Shimada, et al., Determination of incorporated amounts of poly (ethylene glycol)-derivatized lipids in liposomes for the physicochemical characterization of stealth liposomes, Int. J. Pharm. 203 (1-2) (2000) 255–263.
[227] B.M. Discher, et al., Cross-linked polymersome membranes: vesicles with broadly adjustable properties, J. Phys. Chem. B 106 (11) (2002) 2848–2854.
[228] H. Bermudez, et al., Molecular weight dependence of polymersome membrane structure, elasticity, and stability, Macromolecules 35 (21) (2002) 8203–8208.
[229] J.H. Lee, J. Kopecek, J.D. Andrade, Protein-resistant surfaces prepared by PEO-containing block copolymer surfactants, J. Biomed. Mater. Res. 23 (3) (1989) 351–368.
[230] S.I. Ertel, et al., In vitro study of the intrinsic toxicity of synthetic surfaces to cells, J. Biomed. Mater. Res. 28 (6) (1994) 667–675.
[231] J.K. Iyer, et al., Nanodiamonds facilitate killing of intracellular uropathogenic E. coli in an in vitro model of urinary tract infection pathogenesis, PLoS One 13 (1) (2018), e0191020.
[232] J. Ndayishimiye, et al., Nanomaterials: the new antimicrobial magic bullet, ACS Infect. Dis. 8 (4) (2022) 693–712.
[233] N. Chakraborty, et al., Nanobiotics against antimicrobial resistance: harnessing the power of nanoscale materials and technologies, J. Nanobiotechnol. 20 (1) (2022) 375.
[234] R. Saginur, K.N. Suh, Staphylococcus aureus bacteraemia of unknown primary source: where do we stand? Int. J. Antimicrob. Agents 32 (Suppl 1) (2008) S21–S25.
[235] C.L. Ventola, The antibiotic resistance crisis: part 1: causes and threats, Pharm. Therapeut. 40 (4) (2015) 277.
[236] P.S. Stewart, T. Bjarnsholt, Risk factors for chronic biofilm-related infection associated with implanted medical devices, Clin. Microbiol. Infect. (2020).
[237] S. Danti, et al., Applications of bioresorbable polymers in skin and eardrum, Bioresorbable Polym. Biomed. Appl. (2017) 423–444.
[238] E. Fuchs, Scratching the surface of skin development, Nature 445 (7130) (2007) 834–842.
[239] K. Braun, et al., Membrane interactions of mesoporous silica nanoparticles as carriers of antimicrobial peptides, J. Colloid Interface Sci. 475 (2016) 161–170.
[240] S.I. Hay, et al., Measuring and mapping the global burden of antimicrobial resistance, BMC Med. 16 (1) (2018) 1–3.
[241] S. Mukhopadhyay, et al., Antimicrobial peptide polymers: no escape to ESKAPE pathogens—a review, World J. Microbiol. Biotechnol. 36 (9) (2020) 131.
[242] J. Jenkins, et al., Antibacterial effects of nanopillar surfaces are mediated by cell impedance, penetration and induction of oxidative stress, Nat. Commun. 11 (1) (2020) 1–14.

[243] S.J. Kim, et al., The potential role of polymethyl methacrylate as a new packaging material for the implantable medical device in the bladder, Biomed. Res. Int. 2015 (2015), 852456.
[244] J.M. Spanjers, B. Städler, Cell membrane coated particles, Adv. Biosyst. 4 (11) (2020), 2000174.
[245] C.G. Millán, D.G. Bravo, J.M. Lanao, New erythrocyte-related delivery systems for biomedical applications, J. Drug Delivery Sci. Technol. 42 (2017) 38–48.
[246] C.-M.J. Hu, et al., Erythrocyte membrane-camouflaged polymeric nanoparticles as a biomimetic delivery platform, Proc. Natl Acad. Sci. 108 (27) (2011) 10980–10985.
[247] W. Chen, et al., Coating nanofiber scaffolds with beta cell membrane to promote cell proliferation and function, Nanoscale 8 (19) (2016) 10364–10370.
[248] R.H. Fang, et al., Cancer cell membrane-coated nanoparticles for anticancer vaccination and drug delivery, Nano Lett. 14 (4) (2014) 2181–2188.
[249] A. Parodi, et al., Synthetic nanoparticles functionalized with biomimetic leukocyte membranes possess cell-like functions, Nat. Nanotechnol. 8 (1) (2013) 61–68.
[250] W. Di, et al., Real-time particle-by-particle detection of erythrocyte-camouflaged microsensor with extended circulation time in the bloodstream, Proc. Natl Acad. Sci. 117 (7) (2020) 3509–3517.
[251] J. Li, et al., Seedless preparation of Au nanorods by hydroquinone assistant and red blood cell membrane camouflage, RSC Adv. 8 (38) (2018) 21316–21325.
[252] C. Wang, et al., Pretreated macrophage-membrane-coated gold nanocages for precise drug delivery for treatment of bacterial infections, Adv. Mater. 30 (46) (2018), 1804023.
[253] J. Li, et al., Biomimetic platelet-camouflaged nanorobots for binding and isolation of biological threats, Adv. Mater. 30 (2) (2018), 1704800.
[254] K. Chen, et al., Intrinsic biotaxi solution based on blood cell membrane cloaking enables fullerenol thrombolysis in vivo, ACS Appl. Mater. Interfaces 12 (13) (2020) 14958–14970.
[255] V. Vijayan, S. Uthaman, I.-K. Park, Cell membrane coated nanoparticles: an emerging biomimetic nanoplatform for targeted bioimaging and therapy, Biomimetic Med. Mater. (2018) 45–59.
[256] Y. Chen, et al., Broad-spectrum neutralization of pore-forming toxins with human erythrocyte membrane-coated nanosponges, Adv. Healthc. Mater. 7 (13) (2018), 1701366.
[257] J.N. O'Sullivan, et al., Protecting the outside: biological tools to manipulate the skin microbiota, FEMS Microbiol. Ecol. (6) (2020) 96.
[258] S. Tan, et al., Cell or cell membrane-based drug delivery systems, Theranostics 5 (8) (2015) 863.
[259] S. Aryal, C.-M.J. Hu, L. Zhang, Polymeric nanoparticles with precise ratiometric control over drug loading for combination therapy, Mol. Pharmaceutics 8 (4) (2011) 1401–1407.
[260] M.F. Gómez-Núñez, et al., Nanoparticle-based devices in the control of antibiotic resistant bacteria, Front. Microbiol. 11 (2987) (2020).
[261] M. Milazzo, et al., Biodegradable polymeric micro/nano-structures with intrinsic antifouling/antimicrobial properties: relevance in damaged skin and other biomedical applications, J. Funct. Biomater. 11 (3) (2020).
[262] O'Neill, J., Tackling drug-resistant infections globally: final report and recommendations. 2016.
[263] E.D. Brown, G.D. Wright, Antibacterial drug discovery in the resistance era, Nature 529 (7586) (2016) 336–343.
[264] M.A. Watson, S.L. Cockroft, Man-made molecular machines: membrane bound, Chem. Soc. Rev. 45 (22) (2016) 6118–6129.
[265] T. Xu, et al., Fuel-free synthetic micro-/nanomachines, Adv. Mater. 29 (9) (2017), 1603250.
[266] V. García-López, et al., Unimolecular submersible nanomachines. Synthesis, actuation, and monitoring, Nano Lett. 15 (12) (2015) 8229–8239.
[267] H. Yigit, et al., Novel carbapenem-hydrolyzing β-lactamase, KPC-1, from a carbapenem-resistant strain of Klebsiella pneumoniae, Antimicrob. Agents Chemother. 45 (4) (2001) 1151–1161.
[268] E. Smith Moland, et al., Plasmid-mediated, carbapenem-hydrolysing β-lactamase, KPC-2, in Klebsiella pneumoniae isolates, J. Antimicrob. Chemother. 51 (3) (2003) 711–714.
[269] N. Woodford, et al., Outbreak of Klebsiella pneumoniae producing a new carbapenem-hydrolyzing class A β-lactamase, KPC-3, in a New York medical center, Antimicrob. Agents Chemother. 48 (12) (2004) 4793–4799.
[270] D.M. Livermore, Has the era of untreatable infections arrived? J. Antimicrob. Chemother. 64 (suppl_1) (2009) i29–i36.
[271] T. Galbadage, et al., Molecular nanomachines disrupt bacterial cell wall, increasing sensitivity of extensively drug-resistant klebsiella pneumoniae to meropenem, ACS Nano 13 (12) (2019) 14377–14387.
[272] F.D. Halstead, et al., Antimicrobial dressings: Comparison of the ability of a panel of dressings to prevent biofilm formation by key burn wound pathogens, Burns 41 (8) (2015) 1683–1694.
[273] Z. Fan, et al., A novel wound dressing based on Ag/graphene polymer hydrogel: effectively kill bacteria and accelerate wound healing, Adv. Funct. Mater. 24 (25) (2014) 3933–3943.
[274] F. Furno, et al., Silver nanoparticles and polymeric medical devices: a new approach to prevention of infection? J. Antimicrob. Chemother. 54 (6) (2004) 1019–1024.
[275] N. Durán, et al., Antibacterial effect of silver nanoparticles produced by fungal process on textile fabrics and their effluent treatment, J. Biomed. Nanotechnol. 3 (2) (2007) 203–208.
[276] I.E.M. Carpio, et al., Toxicity of a polymer–graphene oxide composite against bacterial planktonic cells, biofilms, and mammalian cells, Nanoscale 4 (15) (2012) 4746–4756.
[277] Z. Meran, et al., Antifungal properties and biocompatibility of silver nanoparticle coatings on silicone maxillofacial prostheses in vitro, J. Biomed. Mater. Res. Part B: Appl. Biomater. 106 (3) (2018) 1038–1051.
[278] K. Naik, M. Kowshik, Anti-quorum sensing activity of AgCl-TiO2 nanoparticles with potential use as active food packaging material, J. Appl. Microbiol. 117 (4) (2014) 972–983.
[279] M.F. Gómez-Núñez, et al., Nanoparticle-based devices in the control of antibiotic resistant bacteria, Front. Microbiol. (2020) 2987.
[280] J.A. Teixeira, et al., Effects of a new nano-silver fluoride-containing dentifrice on demineralization of enamel and streptococcus mutans adhesion and acidogenicity, Int. J. Dentistry 2018 (2018).
[281] J.S. Fernandez-Moure, et al., Nanoantibiotics: a new paradigm for the treatment of surgical infection, Nanomedicine 12 (11) (2017) 1319–1334.
[282] S. Muzammil, et al., Nanoantibiotics: future nanotechnologies to combat antibiotic resistance, Front. Biosci 10 (2018) 352–374.
[283] P.V. Baptista, et al., Nano-strategies to fight multidrug resistant bacteria—"a battle of the titans, Front. Microbiol. 9 (2018) 1441.
[284] M. Kumar, et al., Futuristic non-antibiotic therapies to combat antibiotic resistance: a review, Front. Microbiol. 12 (2021) 16.
[285] R. Vazquez-Munoz, F.D. Lopez, J.L. Lopez-Ribot, Bismuth nanoantibiotics display anticandidal activity and disrupt the biofilm and cell morphology of the emergent pathogenic yeast Candida auris, Antibiotics 9 (8) (2020) 461.
[286] K.N. Thakkar, S.S. Mhatre, R.Y. Parikh, Biological synthesis of metallic nanoparticles, Nanomed. Nanotechnol. Biol. Med. 6 (2) (2010) 257–262.
[287] A.T. Khalil, et al., Sageretia thea (Osbeck.) mediated synthesis of zinc oxide nanoparticles and its biological applications, Nanomedicine 12 (15) (2017) 1767–1789.
[288] A.T. Khalil, et al., Sageretia thea (Osbeck.) modulated biosynthesis of NiO nanoparticles and their in vitro pharmacognostic, antioxidant and cytotoxic potential, Artif. Cells, Nanomed., Biotechnol. 46 (4) (2018) 838–852.
[289] R. Emmanuel, et al., Antimicrobial efficacy of drug blended biosynthesized colloidal gold nanoparticles from Justicia glauca against oral pathogens: a nanoantibiotic approach, Microb. Pathog. 113 (2017) 295–302.
[290] A.N. Grace, K. Pandian, Antibacterial efficacy of aminoglycosidic antibiotics protected gold nanoparticles—a brief study, Colloids Surf. A 297 (1-3) (2007) 63–70.
[291] P. Elia, et al., Green synthesis of gold nanoparticles using plant extracts as reducing agents, Int. J. Nanomed. 9 (2014) 4007.
[292] L. Wang, et al., Functionalised nanoparticles complexed with antibiotic efficiently kill MRSA and other bacteria, Chem. Commun. 50 (81) (2014) 12030–12033.
[293] N. Tarrat, et al., The gold/ampicillin interface at the atomic scale, Nanoscale 7 (34) (2015) 14515–14524.

[294] L.B. Capeletti, et al., Tailored silica–antibiotic nanoparticles: overcoming bacterial resistance with low cytotoxicity, Langmuir 30 (25) (2014) 7456–7464.
[295] S.H. Jun, et al., Silver nanoparticles synthesized using caesalpinia sappan extract as potential novel nanoantibiotics against methicillin-resistant Staphylococcus aureus, J. Nanosci. Nanotechnol. 15 (8) (2015) 5543–5552.
[296] Y. Xie, et al., Gold nanoclusters for targeting methicillin-resistant Staphylococcusaureus invivo, Angew. Chem. Int. Ed Engl. 57 (15) (2018) 3958–3962.
[297] A.D. Durnev, et al., Evaluation of genotoxicity and reproductive toxicity of silicon nanocrystals, Bull. Exp. Biol. Med. 149 (4) (2010) 445–449.
[298] F. Chen, et al., Cellular toxicity of silicon carbide nanomaterials as a function of morphology, Biomaterials 179 (2018) 60–70.
[299] S. Danti, et al., Chitin nanofibril application in tympanic membrane scaffolds to modulate inflammatory and immune response, Pharmaceutics 13 (9) (2021).
[300] I.A. Hoell, G. Vaaje-Kolstad, V.G.H. Eijsink, Structure and function of enzymes acting on chitin and chitosan, Biotechnol. Genet. Eng. Rev. 27 (1) (2010) 331–366.
[301] S. Preetam, et al., Emergence of microfluidics for next generation biomedical devices, Biosens. Bioelectronics: X (2022), 100106.
[302] S.Y. Choi, et al., Microbial polyhydroxyalkanoates and nonnatural polyesters, Adv. Mater. 32 (35) (2020), 1907138.
[303] Y. Zheng, et al., Engineering biosynthesis of polyhydroxyalkanoates (PHA) for diversity and cost reduction, Metab. Eng. 58 (2020) 82–93.
[304] P.C. Ray, H. Yu, P.P. Fu, Toxicity and environmental risks of nanomaterials: challenges and future needs, J. Environ. Sci. Health C 27 (1) (2009) 1–35.
[305] A. Sarma, et al., Therapeutic nanostructures and nanotoxicity, J. Appl. Toxicol. 41 (10) (2021) 1494–1517.
[306] H.L. Karlsson, et al., Copper oxide nanoparticles are highly toxic: a comparison between metal oxide nanoparticles and carbon nanotubes, Chem. Res. Toxicol. 21 (9) (2008) 1726–1732.
[307] B. Wang, et al., Physicochemical origin for free radical generation of iron oxide nanoparticles in biomicroenvironment: catalytic activities mediated by surface chemical states, J. Phys. Chem. C 117 (1) (2013) 383–392.
[308] W.F. Vevers, A.N. Jha, Genotoxic and cytotoxic potential of titanium dioxide (TiO2) nanoparticles on fish cells in vitro, Ecotoxicol. 17 (5) (2008) 410–420.
[309] M. Valko, et al., Free radicals, metals and antioxidants in oxidative stress-induced cancer, Chem. Biol. Interact. 160 (1) (2006) 1–40.
[310] B.K. Nahak, et al., Advances in organ-on-a-chip materials and devices, ACS Appl. Bio Mater. (2022).
[311] S. Preetam, et al., Application of nanobiosensor in health care sector, Bio-Nano Interface (2022) 251–270.
[312] I.E. Mba, E.I. Nweze, Nanoparticles as therapeutic options for treating multidrug-resistant bacteria: research progress, challenges, and prospects, World J. Microbiol. Biotechnol. 37 (6) (2021) 1–30.
[313] M. Huq, Green synthesis of silver nanoparticles using Pseudoduganella eburnea MAHUQ-39 and their antimicrobial mechanisms investigation against drug resistant human pathogens, Int. J. Mol. Sci. 21 (4) (2020) 1510.
[314] Y. Dong, et al., Antibacterial activity of silver nanoparticles of different particle size against Vibrio Natriegens, PLoS One 14 (9) (2019), e0222322.
[315] X. Hu, T.J. Kandasamy Saravanakumar, M.-H. Wang, Mycosynthesis, characterization, anticancer and antibacterial activity of silver nanoparticles from endophytic fungus Talaromyces purpureogenus, Int. J. Nanomed. 14 (2019) 3427.
[316] H. Singh, et al., Ecofriendly synthesis of silver and gold nanoparticles by Euphrasia officinalis leaf extract and its biomedical applications, Artif. Cells, Nanomed., Biotechnol. 46 (6) (2018) 1163–1170.
[317] F. Faghihzadeh, et al., Kinetic, metabolic and macromolecular response of bacteria to chronic nanoparticle exposure in continuous culture, Environ. Sci.: Nano 5 (6) (2018) 1386–1396.
[318] S.T. Khan, J. Musarrat, A.A. Al-Khedhairy, Countering drug resistance, infectious diseases, and sepsis using metal and metal oxides nanoparticles: current status, Colloids Surf. B Biointerfaces 146 (2016) 70–83.
[319] C.A. Dos Santos, et al., Silver nanoparticles: therapeutical uses, toxicity, and safety issues, J. Pharm. Sci. 103 (7) (2014) 1931–1944.
[320] H.A. Hemeg, Nanomaterials for alternative antibacterial therapy, Int. J. Nanomed. 12 (2017) 8211.
[321] Z. Lin, N.A. Monteiro-Riviere, J.E. Riviere, Pharmacokinetics of metallic nanoparticles, Wiley Interdiscip. Rev. Nanomed. Nanobiotechnol. 7 (2) (2015) 189–217.
[322] A.M. Grumezescu, Nanoscale fabrication, optimization, Scale-Up and Biological Aspects of Pharmaceutical Nanotechnology, William Andrew, 2017.
[323] S. Hua, et al., Current trends and challenges in the clinical translation of nanoparticulate nanomedicines: pathways for translational development and commercialization, Front. Pharmacol. 9 (2018) 790.
[324] K.M. Varier, et al., Nanoparticles: antimicrobial applications and its prospects, in: M. Remediation, S. Naushad (Eds.), Advanced Nanostructured Materials for Environmental, Springer International Publishing, Cham, 2019, pp. 321–355. Rajendran, and F. Gracia, Editors.